Simple and accurate methodology for quantification of genetic markers in acute leukemias and myeloproliferative neoplasms

急性白血病と骨髄増殖性腫瘍における遺伝子マーカーの
簡便・正確な定量手法

February 2011

Waseda University
Graduate School of Advanced Science and Engineering,
Major in Life Science and Medical Bioscience

Soji Morishita

森下　総司

JUDGING COMITTEE

Referee in chief:

Professor Dr. Satoshi Tsuneda

(Dept. of Life Science and Medical Bioscience, Waseda University)

Referees:

Professor Dr. Yasuo Ikeda

(Dept. of Life Science and Medical Bioscience, Waseda University)

Professor Dr. Takashi Kato

(Dept. of Biology, Waseda University)

Professor Dr. Norio Komatsu

(Dept. of Hematology, Juntendo University School of Medicine)

Contents

Chapter 1

General Introduction

Chapter 2

Rapid and simple quantification method targeting WT1 mRNA for the minimal residual disease monitoring in acute leukemias

Chapter 3

Simple, cost-effective, and accurate JAK2 allele burden quantification for the myeloproliferative neoplasms

Chapter 4

Digital PCR is appropriate as the primary measurement of the standard samples for nucleic acid quantification

Chapter 1

General Introduction

Chapter 1

General Introduction

1

1.1. Background and objectives

Biomarkers are defined as materials that reflect or indicate the existence of particular diseases or the condition in the body. Various materials can be candidate of the biomarker such as nucleic acids, peptides, proteins, and lipid metabolites. In particular, biomarkers of nucleic acids (genetic markers) are relatively easily detected and/or quantified owing to the development and diffusion of nucleic acid quantification methods [1-5]. Therefore, genetic markers are now being employed in the clinical fields as diagnostics of the diseases, prognostics of the therapy, and the monitoring of the minimal residual disease (MRD). These trials are aggressively performed in the cancer therapies, especially in the hematopoietic malignancies. For example, *BCR/ABL* chimeric gene is observed in >90% of the patients with chronic myeloid leukemia (CML) [6-8]. *BCR/ABL* chimeric gene is therefore a powerful genetic marker for the diagnostic of CML. Also, the chimeric gene can be used as a marker of the effective drug selection by detecting the point mutations at the ABL kinase domain, and helps prognostic of the therapy. Moreover, *BCR/ABL* chimeric gene is used for the monitoring of the MRD after the administration of several molecular-targeted drugs such as

imatinib [9]. As described above, genetic markers are used not only as the marker for the diagnostic of the diseases but also as the prognostic of the therapy and the monitoring of the diseases. Here, it is expected that the screening and the identification of novel genetic markers, and the methods for detection and/or quantification of identified genetic markers would be in the important position. In fact, newly developed comprehensive genome analysis enabled us to explore and discover novel genetic markers in a few decades [10, 11]. Along with the findings, the quantification of the genetic markers is highly needed in terms of the definite diagnosis, the disease prognosis, and the MRD monitoring.

In this study, the genetic markers of acute leukemias and myeloproliferative neoplasms were focused on. The objective of this study is to construct the quantification methods for these genetic markers. In acute leukemias, a messenger ribonucleic acid (mRNA), Wilms' tumor gene 1 mRNA (WT1 mRNA), is overexpressed in the patients with leukemia in comparison with the healthy donors [12] (Chapter 2). On the other hand, a point gene mutation in Janus kinase gene 2 (*JAK2*) is reported in the myeloproliferative neoplasms [13-15] (Chapter 3 and 4). These two types cover the almost of genetic markers; therefore, the procedures constructed on this study would be able to be applied on other genetic markers (Figure 1.1).

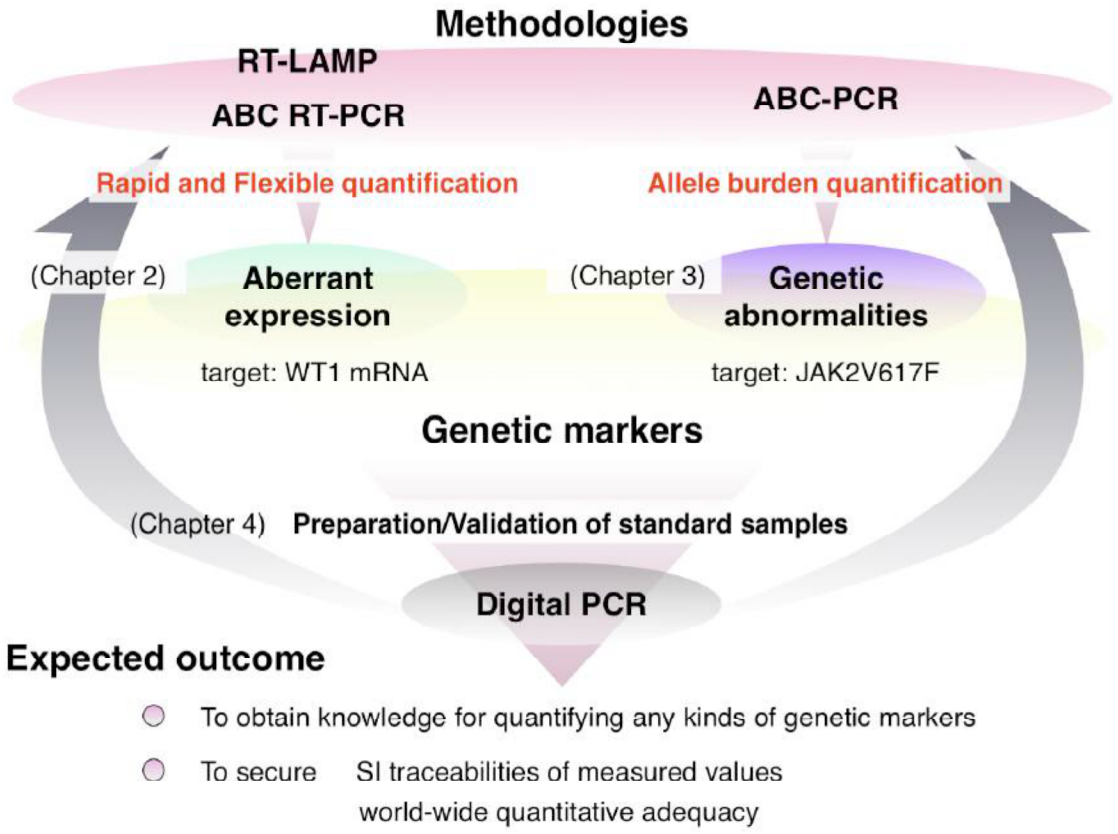

Figure 1.1. Overview of this study

1.2. Genetic markers

In the section, genetic markers of the acute leukemias and the myeloproliferative neoplasms are described. I also focus on the role of the transcripts of these genetic markers in each disease.

1.2.1. Genetic markers for acute leukemia

In acute type leukemias, leukemia type-specific fusion genetic markers such as *AML1/ETO*, *CBFβ/MYH11*, and *PML/RARα* were reported [16-18]. However, more than 50% of all acute myeloid leukemia (AML) samples lack one of these specific fusion genes. Hence, it is crucial to find more universal molecular targets for MRD detection and quantification in leukemia. In 1994, Inoue et al. reported that the WT1 mRNA was aberrantly expressed in patients with various types of leukemias thereby the mRNA would be expected as a promising pan-leukemia genetic marker [12].

The WT1 gene was isolated as a gene responsible for a pediatric renal cancer, Wilms' tumor. The WT1 gene encodes 10 exons and generates a 3 kb mRNA [19, 20]. WT1 mRNA encodes four zinc-finger transcription factors affecting the cell proliferation and differentiation, apoptosis and organ development [21]. Although the WT1 gene had been originally defined as a tumor suppressor gene, the gene seemed to play an oncogenic role rather than a tumor suppressor in leukemias. Based on the actual status, the MRD monitoring method for AML had been developed by quantifying the expression level of WT1 mRNA [21]. The method is based on the quantitative reverse transcription polymerase chain reaction (qRT-PCR) and the expression level of WT1 mRNA in the peripheral blood sample is quantified. The lower limit of the quantification of this method is determined as 50 copies/μg of total RNA. In 2007, the

method was covered by insurance in Japan; therefore, the quantification of the WT1 mRNA expression level is usually performed in terms of the follow up after the therapies. Furthermore, since the WT1 mRNA is aberrantly expressed in patients with leukemias, the WT1 is expected as a candidate for immunotherapy [22, 23]. Some research groups reported that the WT1 peptide vaccination was effective on the patients with AML or myelodysplastic syndrome (MDS) [22, 23].

It is yet unclear how WT1 affects the kinetics of leukemia [21], but Wagner et al. showed that the WT1 might affect the vascularization in solid tumors [24]. In the study, it was suggested that transcriptional activation of tumor angiogenesis factor, ETS-1, by the WT1 is a crucial step in tumor vascularization via regulation of endothelial cell proliferation and migration [24]. Moreover, WT1 mRNA was regulated by the hypoxia-inducible factor 1 (HIF-1) [25]. Therefore, it is considered that the vascularization of tumor cells is regulated as follows: first, HIF-1 is induced by the hypoxic condition of the tumor cells, then WT1 mRNA is overexpressed via HIF-1, finally ETS-1 is regulated by WT1. Think around the case of leukemias, MRDs usually remain in the depth of the bone marrow, which is under the hypoxic condition thereby HIF-1 is possibly expressed in MRDs. As described above, HIF-1 regulates the expression of WT1 mRNA; therefore, WT1 might affect the tumorigenesis of hematopoietic cells. However, no reports exist that clarifies the relationship of WT1 and hematopoietic cells.

1.2.2. Genetic markers for myeloproliferative neoplasms

The discovery of *JAK2* point mutation at *JAK2* exon 14 was the first break in myeloproliferative neoplasms (MPNs) expect for CML [13-15]. After the findings, various gene deletions or mutations were reported by use of comprehensive genome analysis methods such as microarrays and pyrosequencing [10, 11]. In this subsection, *JAK2* mutations and mutations other than *JAK2*, and also their roles in MPNs are described.

1.2.2.1. JAK2 mutations

Two mainly *JAK2* mutations in MPNs, essential thrombocythemia (ET), polycythemia vera (PV), and primary myelofibrosis (PMF), are discovered up to date. One is a somatic *JAK2* point mutation, JAK2V617F [13-15]. The JAK2V617F is the alteration of the guanine base (G) to the thymine base (T) in the locus of the 73rd base of the exon 14. The reported JAK2V617F is found in 45% of patients with ET, in 95% with PV, and in ~50% with PMF [26]. JAK2 is a non-reporter tyrosine kinase. JAK2 has been implicated in signaling by the single chain receptors (e.g. Epo-R; erythropoietin receptor, Tpo-R; thrombopoietin receptor). JAK2 regulates the hematopoiesis thorough the phosphorylation of several signal transductions (e.g. the signal transducers and activator of transcription). JAK2V617F locates on the JH2 domain that negatively regulates the JAK2 kinase activity [27]. Therefore, the mutation triggers the homeostatic activation of the JAK2, which results in the overexpression of several hematopoietic cells [28]. Along with these findings, detection of JAK2V617F was added into one of the major criteria for MPNs diagnosis of the 2008 world health organization (WHO) classification (Figure 1.2).

Polycythemia vera		
Major criteria	1	Hemoglobin >18.5 g/dL in men, 16.5 g/dL in women or other evidence of increased red cell volume * Hemoglobin or hematocrit greater than 99th percentile of method-specific reference range for age, sex, altitude of residence * Hemoglobin >17 g/dL in men, 15 g/dL in women if associated with a documented and sustained increase of at least 2 g/ dL from an individual's baseline value that can not be attritude to correction of iron deficiency * Elevated red cell mass greater than 25% above mean normal predicted value
	2	Presence of JAK2V617F or other functionally similar mutation such as JAK2 exon 12 mutation
Minor criteria	1	Bone marrow biopsy showing hypercellularity for age with trilineage growth (panmyelosis) with prominent erythloid, granulocytic, and megakaryocytic proliferation
	2	Serum erythlopoietin level below the reference range of normal
	3	Endogenous erythloid colony formation *in vitro*
Note:		Diagnosis requires the presence of both major criteria and 1 minor criterion or the presence of the first major criterion together with 2 minor criteria.

Essential thrombocythemia		
	1	Sustained platelet count ≥450000/μL
	2	Bone marrow biopsy specimen showing proliferation mainly of the megakaryocytic lineage with increased number of enlarged, mature megakaryocytes; no significant increase or left-shift of neutrophil granulopoiesis or erythlopoiesis
	3	Not meeting WHO criteria for PV, PMF, CML, MDS, or other myeloid neoplasm
	4	Demonstration of JAK2V617F or other clonal marker, or in the absence of a clonal marker, no evidence for reactive thrombocytosis
Note:		Diagnosis requires meeting all 4 criteria.

Primary myelofibrosis		
Major criteria	1	Presence of megakaryocyte proliferation and atypia, usually accompanied by either reticulin and/or collagen fibrosis, or, in the absence of significant reticulin fibrosis, the megakaryocyte changes must be accompanied by an increased bone marrow cellularity characterized by granulocytic proliferation and often decreased erythlopoiesis (i.e. prefibrotic cellular-phase disease)
	2	No meeting WHO criteria for PV, CML, MDS, or other myeloid neoplasm
	3	Demonstration of JAK2V617F or other clonal marker (e.g. MPLW515L/K), or in the absence of a clonal marker, no evidence of bone marrow fibrosis due to underlying inflammatory or other neoplastic diseases
Minor criteria	1	Leukoerythroblastosis
	2	Increase in serum lactate dehydrogenase level
	3	Anemia
	4	Palpable splenomegary
Note:		Diagnosis requires meeting all 3 major criteria and 3 minor criteria.

Figure 1.2. Criteria for MPNs diagnosis of the 2008 WHO classification

The other mutation is *JAK2* exon 12 mutation [29]. The mutation has a various types of mutations including repetition or deletion of certain sequences. The mutational variation was reported as a rare case of European patients; however, it was also reported that the mutational variation was often detected in Asian patients [30].

1.2.2.2. Mutations other than JAK2

As described above, JAK2V617F is not detected in approximately half of the patients with ET and PMF. Exploration of other gene mutations than *JAK2* discovered several gene mutations such as *MPL*, *LNK*, and *TET2* [31-33]. *MPL* mutations (MPLW515L/K) occur to the Tpo-R. The Tpo-R regulates the differentiation of megakaryocytes through the binding of thrombopoietin (TPO). Therefore, it is considered that MPLW515L/K trigger the homeostatic activation of Tpo-R and then the homeostatic activated Tpo-R results in the overexpression of megakaryocytes. MPLW515L/K are detected in >5% of ET, and 10% of PMF but are not detected in PV [31]. LNK is an adapter protein that has SH2 domain and pleckstrin homology (PH) domain. The protein negatively regulates the JAK/STAT signaling after the stimulation of TPO [34]. In 2010, Oh et al. identified the *LNK* mutations [32]. They reported that the *LNK* mutations were detected 1/14 in ET, 1/18 in PMF. In the study, *LNK* mutation in ET was a point mutation of the guanine to cytosine alternation, caused E208Q alternation of the amino acids. The mutation in PMF caused deletion of both SH2 and PH domains in LNK. Both two *LNK* mutations induced the excessive activation of the JAK/STAT signaling [32]. *TET2* mutations were found in 2009 and several deletions and mutations of the gene were detected in MPNs [33]. The mechanism of TET2 had been unclear; however, it was reported that 5-methylcytosine on mammalian DNA was converted to 5-hyroxymethylcytosine by TET1 [35]. It has been suggested that TET2 also has such

epigenetic function because both TET1 and TET2 are in the TET family. Then, sure enough, Jankowska et al. more recently indicated that mutated TET2 caused the epigenetic abnormality and triggered MPNs [36].

As described above, various type of gene mutations have been detected in MPNs, and moreover, the role of these gene mutations are becoming clear owing to the contribution of the recent researches (Figure 1.3). In the soon future, the researches about the correlation between gene mutation ratio and the diseases would be conducted.

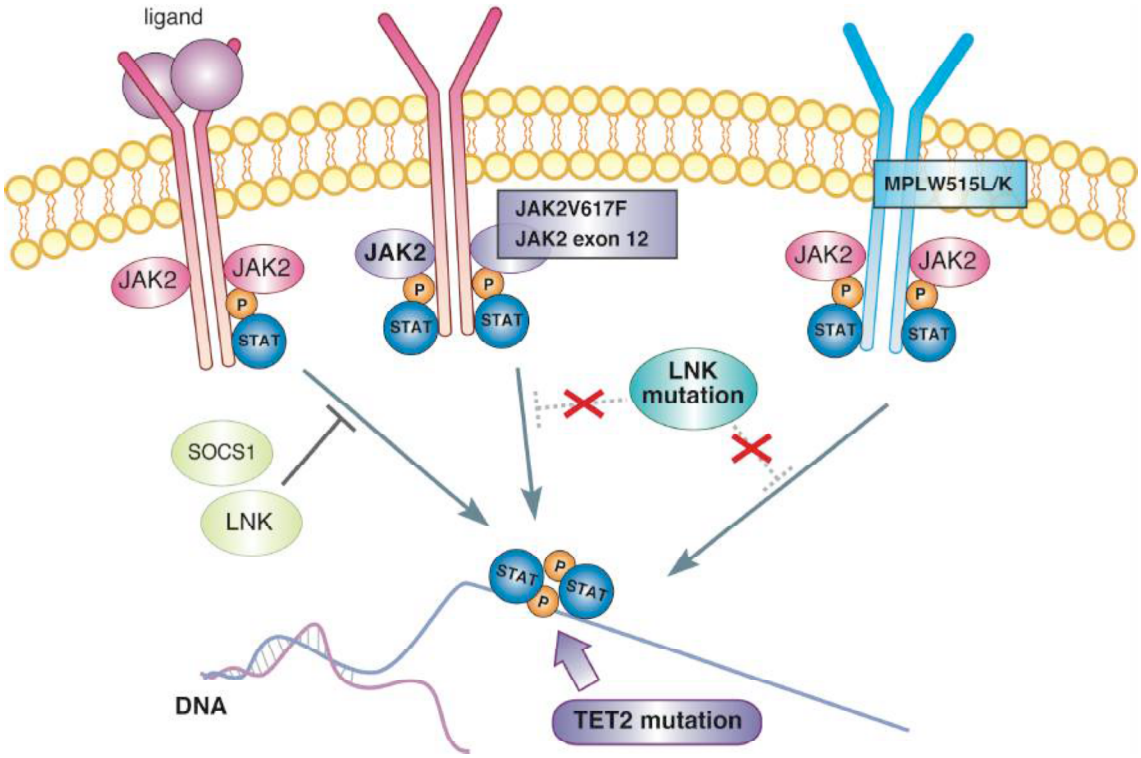

Figure 1.3. The role of mutated proteins in MPN

1.3. Nucleic acids quantification methods

In this study, the quantification methods for WT1 mRNA and JAK2V617F are established utilizing Loop-mediated isothermal amplification (LAMP) [37], Alternately binding probe Competitive PCR (ABC-PCR) [38], and digital PCR [40]. The principle of each method is described below.

1.3.1. LAMP

LAMP is an isothermal DNA amplification method that is performed at ranging from 60-65ºC in a short time (15-60 min) [37]. The method relies on autocycling strand displacement DNA synthesis by the *Bst* DNA polymerase with a set of three outer and inner primers (Figure 1.4), guaranteeing the specificity of LAMP [41, 42]. The method is able to amplify target sequences to 10^9–10^{10} times within 30 min. The efficiency is approximately 100 times higher than that of PCR. LAMP is also useful for RNA template detection with the use of reverse transcriptase together with DNA polymerase [43, 44]. However, it is quite difficult to define the efficient combination of the primer recognition region and design the sufficient primer set for LAMP. In the case of the quantification utilizing LAMP, real-time turbidimetry LAMP is usually employed [41]. In the real-time turbidimetry LAMP, the turbidity derived from magnesium pyrophosphate, which is a byproduct of LAMP, is monitored in real-time by measuring the absorbance of the aliquot at 650 nm (Figure 1.5).

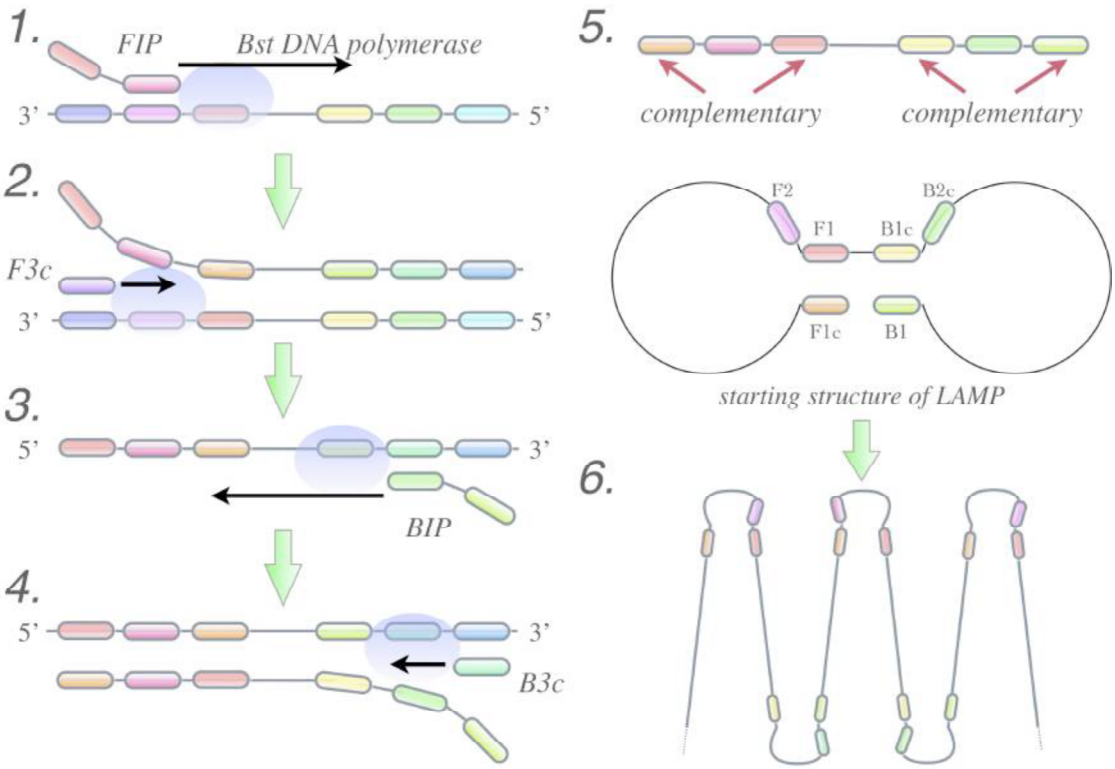

Figure 1.4. Schematic illustration of the LAMP

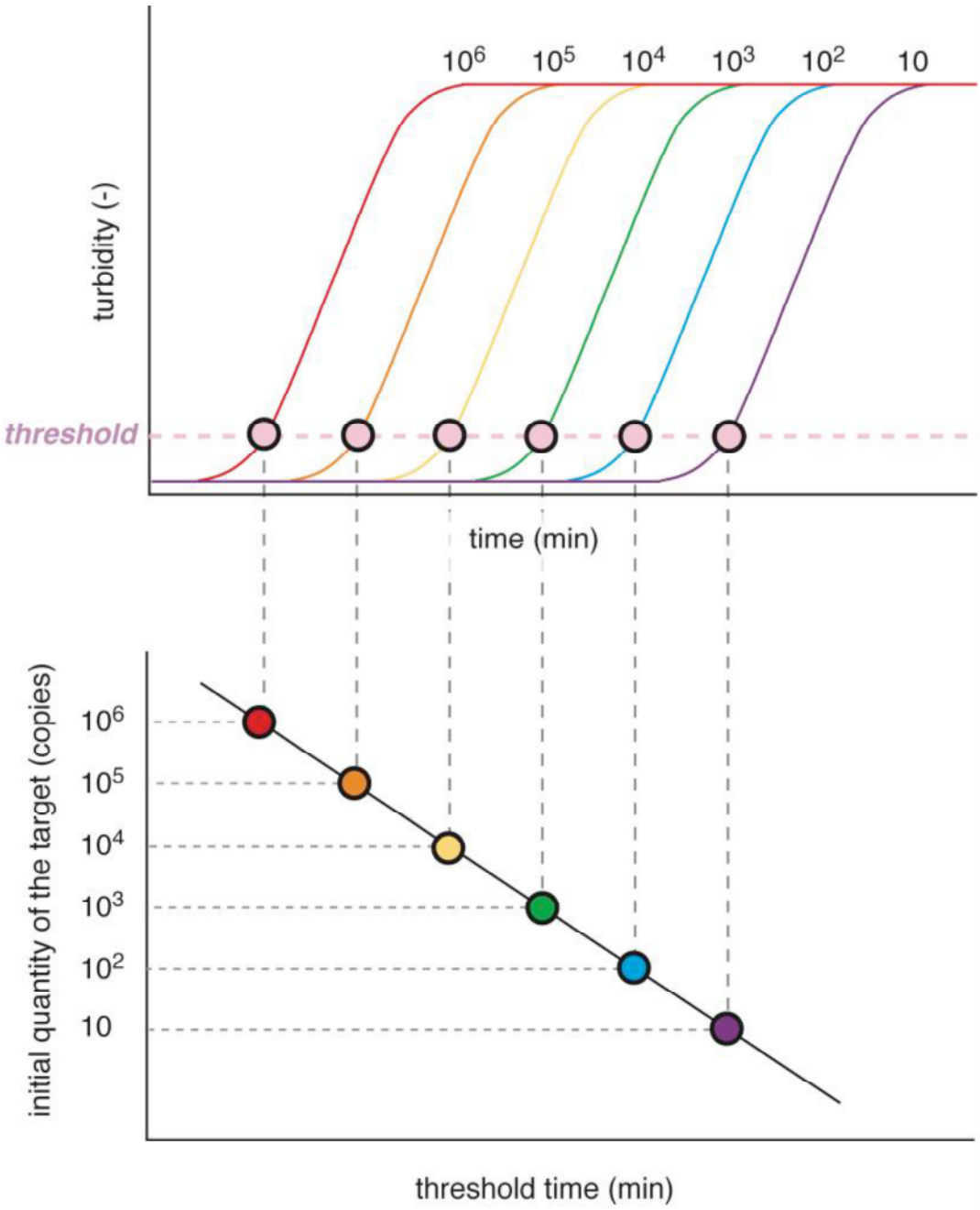

Figure 1.5. real-time turbidimetry LAMP

1.3.2. ABC-PCR

The detailed principle of ABC-PCR is described in the Ph.D. thesis written by Tani [38]. Concisely, ABC-PCR was developed as a reliable quantification of nucleic acids in biological samples that contain PCR inhibitors and eliminates false negative results [39]. A scheme of the ABC-PCR is shown in Figure 1.7. ABC-PCR is the competitive PCR based nucleic acids quantification method. Competitive PCR uses a deoxyribonucleic acid (DNA) or ribonucleic acid (RNA) fragment (competitor) that is coamplified with the gene of interest (target). In competitive PCRs, the ratio of the target to the competitor is maintained. Because the stating quantity of the competitor is known, the starting quantity of the target can be calculated by measuring of the target ratio to the competitor. The target ratio to the competitor is measured by use of a fluorescent probe that binds to either the target or the competitor in ABC-PCR [39]. The fluorescent probe, named alternately binding probe (AB-Probe), is an oligonucleotide with a green dye (BODIPY-FL, excitation/emission = 505/513 nm) at a 5′-end, and a red dye (TAMRA, excitation/emission = 555/580 nm) at a 3′-end. These fluorescent dyes have a property of being notably quenched by the photo-induced electron transfer (PeT) to a guanine base at the particular position [45, 46]. The competitor used for ABC-PCR is identical to the corresponding region of the target except for three bases located outside position of the binding site for the 5′-side of the probe. These three bases are replaced to guanine. Therefore, the fluorescence intensity of the AB-Probe behaves as follows (also shown in Figure 1.6):

(i) When the probe is free in solution, its green fluorescence intensity (G_U) is quenched via fluorescence resonance energy transfer (FRET) to the red dye (R_U).

(ii) When the probe binds to the target, the green fluorescence emits (G_T) because of the reduction of FRET, and the red fluorescence quenches by the effect of PeT to the

guanine base (R_T).

(iii) When the probe binds to the competitor, the green fluorescence is notably quenched (G_C) by the effect of PeT, and the red fluorescence is also quenched (R_C).

Taken together, the green dye reflects the target ratio to the competitor, and the red dye reflects the ratio of the amount of the unbound probe to that of the bound probe.

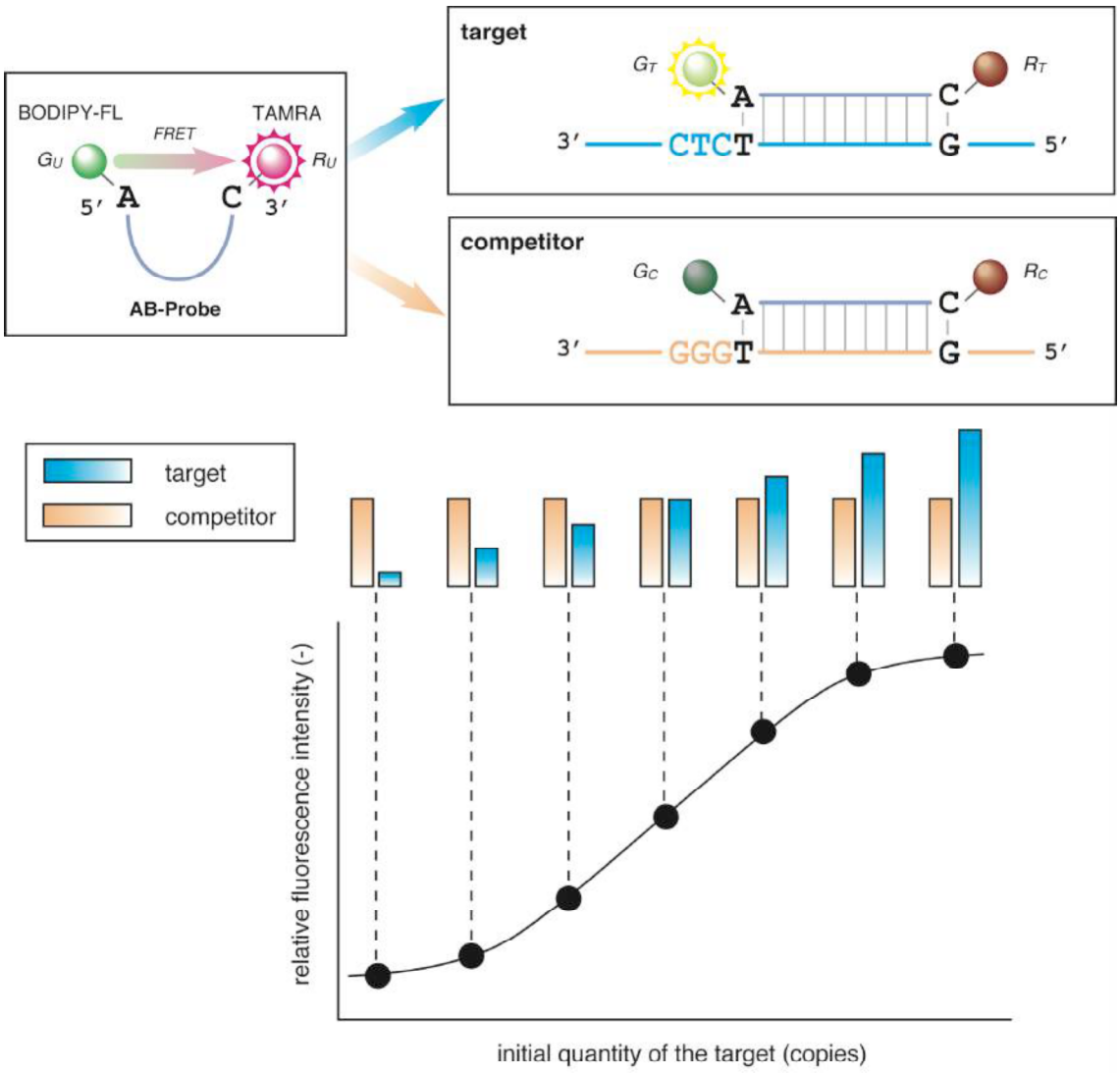

Figure 1.6. Schematic illustration of the ABC-PCR

1.3.3. digital PCR

Digital PCR is a newly developed technology [40], which is performed by the massively parallel nano-litter scaled PCR amplification across a large number of partitions. Each partition contains theoretically 0.5 copies of the target, resulting in binary (i.e. positive/negative) signals. Counting up the positive signals, DNA "absolute" copy number can be estimated (Figure 1.7) [47]. Digital PCR is attracted to the medical field. For example, digital PCR is reported to utilize for the screening of drug resistance in patients with CML by estimating the copy number variation [48] or for the antenatal diagnosis of fetal chromosomal aneuploidy by detecting low copy number DNA sequences in maternal plasma [49]. Because of its quantitative accuracy and sensitivity, the digital PCR is also used for the investigation of the number of library molecules applied to next-generation sequencing [50]. However, the method has limitations at the point of throughput and running cost. Further technological developments are ongoing to overcome these shortcomings [51, 52].

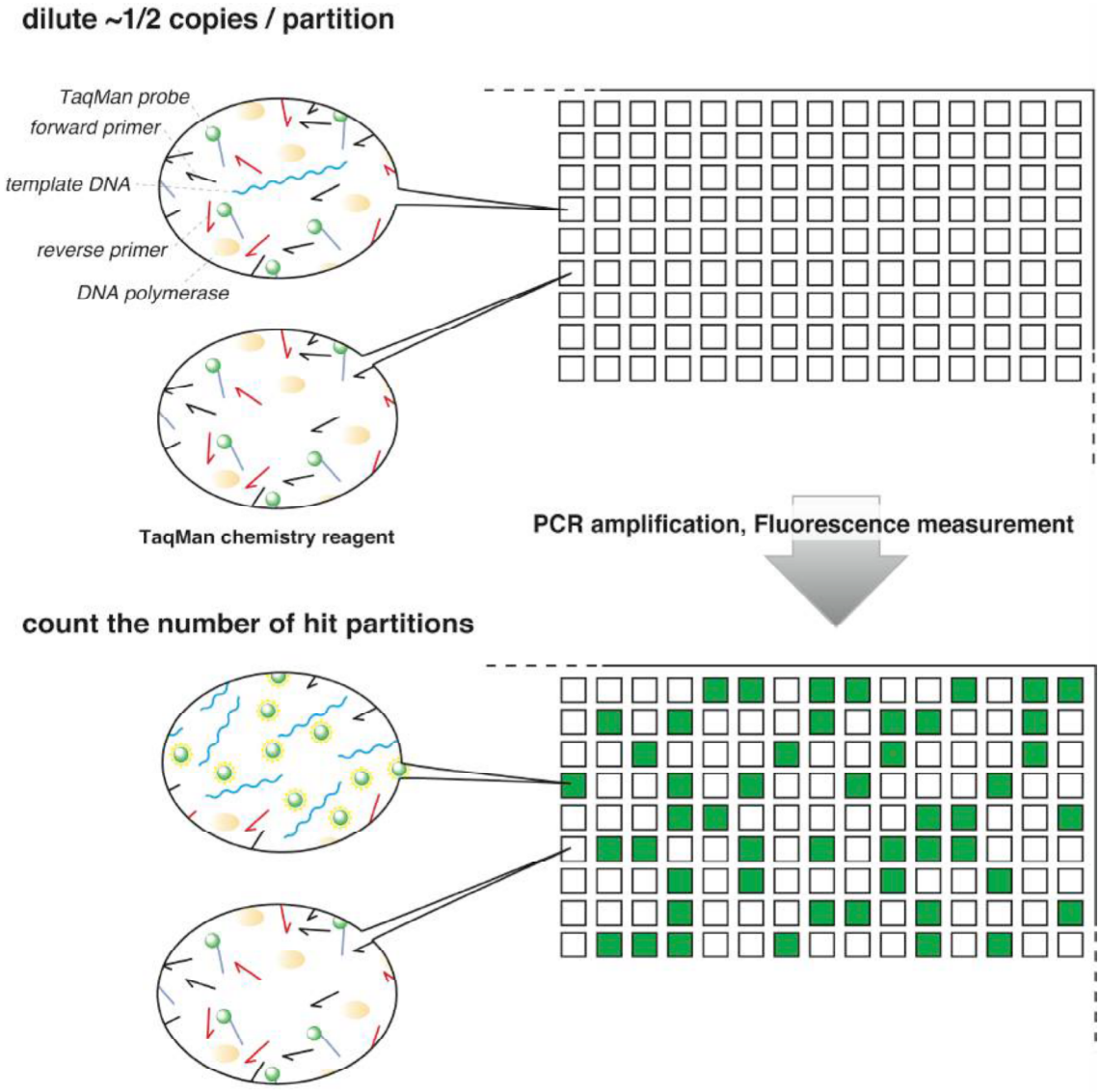

Figure 1.7. Schematic illustration of the digital PCR

References

1. Alwine J. C., Kemp D. J., and Stark G. R. Method for detection of specific RNAs in agarose gel by transfer to diazobenzyloxymethyl-paper and hybridization with DNA probes. *Proc. Nath. Acad. Sci. U.S.A.* 1997; **74:** 5350-4.
2. Morrison T. B., Weis J. J., and Witter C. T. Quantification of low-copy transcripts by continuous SYBR (R) green I monitoring during amplification. *Biotechniques* 1998; **24:** 954-62.
3. Livak K. J., Flood S., J., Marmaro J., Glusti W., and Deetz K. Oligonucleotides with fluorescent dyes at opposite ends provide a quenched probe system useful for detecting PCR product and nucleic acid hybridization. *PCR Methods* 1995; **4:** 357-62.
4. Tyagi S. and Kramer F. R. Molecular beacons: Probes that fluoresce upon hybridization. *Nat. Biotechnol.* 1996; **14:** 303-8.
5. Witter C. T., Hermann M. G., Moss A. A., and Rasmussen R. P. Continuous fluorescence monitoring of rapid cycle DNA amplification. *Biotechniques* 1997; **22:** 130-1.
6. Eder M., Battmer K., Kafert S., Stuscki A., Ganser A., and Hertenstein B. Monitoring of BCR-ABL expression using real-time RT-PCR in CML after bone marrow or peripheral blood stem cell transplantation. *Leukemia* 1999; **13:** 1383-9.
7. Lin F., F. van Rhee, Goldman J. M., and Cross N., C. Kinetics of increasing BCR-ABL transcript numbers in chronic myeloid leukemia patients who relapse after bone marrow transcription. *Blood* 1996; **10:** 4473-8.
8. Olavarria E., Kanfer E., Szydlo R., et al. Early detection of BCR-ABL transcripts by quantitative reverse transcriptase-polymerase chain reaction predicts outcome after allogeneic stem cell transplantation for chronic myeloid leukemia. *Blood*

2001; **15:** 1560-5.

9. Druker B. J., Talpaz M., Resta D. J., et al. Efficiency and safety of a specific inhibitor of the BCR-ABL tyrosine kinase in chronic myeloid leukemia. *N. Engl. J. Med.* 2001; **344:** 1031-7.
10. Schena M., Shalon D., Davis R. W., and Brown P. O. Quantitative monitoring of gene expression patterns with a complementary DNA microarray. *Science* 1995; **270:** 467-70.
11. Voelkerding K. V., Dames S. A., and Durtschi J. D. Next-generation sequencing: From basic research to diagnostics. *Clin. Chem.* 2009; **55:** 641-58.
12. Inoue K., Sugiyama H., Ogawa H., et al. WT1 as a new prognostic factor and a new marker for the detection of minimal residual disease in acute leukemia. *Blood* 1994; **84:** 3071-9.
13. Baxter E. J., Scott L. M., Cambell P. J., et al. Acquired mutation of the tyrosine kinase JAK2 in human myeloproliferative disorders. *Lancet* 2005; **365:** 1054-61.
14. James C, Ugo V., Le Couédic J. P., et al. A unique clonal JAK2 mutation to constitutive signaling causes polycythemia vera. *Nature* 2005; **434:** 1144-8.
15. Levine R. L., Wadleigh M., Cools J., et al. Activating mutation in the tyrosine kinase JAK2 in polycythemia vera, essential thrombocythemia, and myeloid metaplasia with myelofibrosis. *Cancer Cell* 2005; **7:** 387-97.
16. Nucifora G. and Rowley J. D. AML1 and the 8; 21 translocations in acute and chronic myeloid leukemia. *Blood* 1995; **86:** 1-14.
17. Claxton D. F., Liu P., Hsu H. B., et al. Detection of fusion transcripts generated by the inversion 16 chromosome in acute myelogenous leukemia. *Blood* 1994; **83:** 1750-6.
18. Kominger L., Knöbl P., Mustafa S., et al. PML-RARα PCR positivity in the bone

marrow of patients with APL precedes haematological relapse by 2–3 months. *Br. J. Haematol.* 1994; **88:** 427-31.

19. Wagner K. J. and Roberts S. G. E. Transcriptional regulation by the Wilms' tumour suppressor protein WT1. *Biochem. Soc. Trans.* 2004; **32:** 932-5.
20. Yang L., Han Y., Saurez F., and Minden M. D. A tumor suppressor and oncogene: the WT1 story. *Leukemia* 2007; **21:** 868-76.
21. Weisser M., Kern W., Rauhut S., et al. Prognostic impact of RT-PCR based quantification of WT1 gene expression during MRD monitoring of acute myeloid leukemia. *Leukemia* 2005; **19:** 1416-23.
22. Oka Y., Tsuboi A., Oji Y., Kawase I., and Sugiyama H. WT1 peptide vaccine for the treatment of cancer. *Curr. Opin. Immunol.* 2008; **20:** 211-20.
23. Chaise C., Buchan S. L., Rice J., et al. DNA vaccination induces WT1-specific T-cell responses with potential clinical relevance. *Blood* 2008; **112:** 2956-64.
24. Wagner N., Michiels J. F., Schedl A., and Wagner K-D. The Wilms' tumour suppressor WT1 is involved in endothelial cell proliferation and migration: expression in tumour vessels *in vivo*. *Oncogene* 2008; **27:** 3662-72.
25. Wagner K-D., Wagner N., Wellmann S., Schley G., Bondke A., Theres H., and Scholz H. Oxygen-regulated expression of the Wilms' tumor suppressor Wt1 involves hypoxia-inducible factor-1 (HIF-1). *FASEB J.* 2003; **17:** 1364-6.
26. Schnittger S., Backer U., Haferlach C., et al. Detection of JAK2 exon 12 mutations in 15 patients with JAK2V617F negative polycythemia vera. *Haematologica* 2009; **94:** 414-8.
27. Saharainen P., Vihinen M., and Silvennoinen O. Autoinhibition of Jak2 tyrosine kinase is dependent on specific regions in its pseudokinase domain. *Am. Soc. Cell Biol.* 2003; **14:** 1448-59.

28. Campbell P. J. and Green A. R. The myeloproliferative disorders. *N. Engl. J. Med.* 2006; **355:** 2452-66.

29. Scott L. M., Tong W., Levine R. L., et al. JAK2 exon 12 in polycythemia vera and idiopathic erythrocytosis. *N. Engl. J. Med.* 2007; **365:** 459-68.

30. Yeh Y. M., Chen Y. L., Cheng H. Y., et al. High percentage of JAK2 exon 12 mutation in Asian patients with polycythemia vera. *Am. J. Clin. Pathol.* 2010; **134:** 266-70.

31. Pardanani A. D., Levine R. L., Lasho T., et al. MPL515 mutations in myeloproliferative and other myeloid disorders: a study of 1182 patients. *Blood* 2006; **108:** 3472-6.

32. Oh S. T., Simonds E. F., Jones C., et al. Novel mutations in the inhibitory adapter protein LNK drive JAK-STAT signaling in patients with myeloproliferative neoplasms. *Blood* 2010; **116:** 988-92.

33. Delhommeau F., Dupont S., Valle V. D., et al. Mutation in TET2 in myeloid cancers. *N. Engl. J. Med.* 2009; **360:** 2289-2301.

34. Seita J., Ema H., Ooehara J., et al. Lnk negatively regulates selfrenewal of hematopoietic stem cells by modifying thrombopoietin-mediated signal transduction. *Proc. Natl. Acad. Sci. U.S.A.* 2007; **104:** 2349-54.

35. Tahiliani M., Koh K. P., Shen Y., et al. Conversion of 5-methylcytosine to 5-hydroxymethylcytosine in mammalian DNA by MLL partner TET1. *Science* 2009; **324:** 930-5.

36. Jankowska A., Ko M., Huang Y., et al. Impaired hydroxylation of 5-methlcytosine in TET2 mutated patients with myeloid malignancies. American Society of Hematology the 52nd annual meeting, December 5, 2010, FL, USA.

37. Notomi T., Okayama H., Masubuchi H., et al. Loop-mediated isothermal

amplification of DNA. *Nucleic Acids Res.* 2000; **28:** e63.

38. Tani H. Development of quantitative method for specific nucleic acid sequences using fluorescence quenching phenomenon. Ph.D. thesis 2008; Waseda University, Tokyo, Japan.
39. Tani H., Kanagawa K., Kurata S., et al. Quantitative method for specific nucleic acid sequences using competitive polymerase chain reaction with an alternately binding probe. *Anal. Chem.* 2007; **79:** 974-9.
40. Vogelstein B. and Kinzler K. W. Digital PCR. *Proc. Natl. Acad. Sci. U.S.A.* 1999; **96:** 9236-42.
41. Mori Y., Kitao M., Tomita N., and Notomi T. Real-time turbidimetry of LAMP reaction for quantifying template DNA. *Biochem. Biophys. Meth.* 2004; **59:** 145-57.
42. Aoi Y., Hosogai M., and Tsuneda S. Real-time quantitative LAMP (loop-mediated isothermal amplification of DNA) as a simple method for monitoring ammonia-oxidizing bacteria. *J. Biotech.* 2006; **125:** 484-91.
43. Toriniwa H. and Komiya T. Rapid detection and quantification of Japanese encephalitis virus by real-time reverse transcription loop-mediated isothermal amplification. *Microbiol. Immunol.* 2006; **50:** 379-87.
44. Parida M., Posadas G., Inoue S., Hasebe F., and Morita K. Real-time reverse transcription loop-mediated isothermal amplification for rapid detection of West Nile virus. *J. Clin. Microbiol.* 2004; **42:** 257-63.
45. Torimura M., Kurata S., Yamada K., Yokomaku T., Kamagata Y., Kanagawa T., and Kurane R. Fluorescence-quenching phenomenon by photoinduced electron transfer between a fluorescent dye and a nucleic base. *Anal. Sci.* 2001; 17: 155-60.
46. Kurata S., Kanagawa T., Yamada K., Torimura M., Yokomaku T., Kamagata Y.,

and Kurane R. Fluorescent quenching-based quantitative detection of specific DNA/RNA using a BODIPY® FL-labeled probe or primer. *Nucleic Acids Res.* 2001; **29:** e34.

47. Pohl G. and Shie Ie M. Principle and applications of digital PCR. *Expert Rev. Mol. Diagn.* 2004; **4:** 41-7.
48. Ohler V. G., Qin J., Ramakrishnan R., et al. Absolute quantitative detection of ABL tyrosine kinase domain point mutation in chronic myeloid leukemia using a novel nanofluidic platform and mutation-specific PCR. *Leukemia* 2009; **23:** 396-9.
49. Dennis Lo Y. M., Lun F. M. F., Allen Chan K. C., et al. Digital PCR for the molecular detection of fetal chromosomal aneuploidy. *Proc. Natl. Acad. Sci. U.S.A.* 2007; **104:** 13116-21.
50. White R. A. III, Blainey P. C., Fan H. C., and Quake S. R. Digital PCR provides sensitive and absolute calibration for high throughput sequencing. *BMC Genomics* 2009; **10:** 116-27.
51. Zang Y., Novak R., Shuga J., Smith M. T., and Mathies R. A. High-performance single cell genetic analysis using microfluidic emulsion generator arrays. *Anal. Chem.* 2010; **82:** 3183-90.
52. Sandberg S. O., Witter C. T., Gao C., and Gale B. K. Spinning disk platform for microfluidic digital polymerase chain reaction. *Anal. Chem.* 2010; **82:** 1546-50.

Chapter 2

Rapid and simple quantification method targeting WT1 mRNA for the MRD monitoring in acute leukemias

Chapter 2

Rapid and simple quantification method targeting WT1 mRNA for the minimal residual disease monitoring in acute leukemias

2

2.1. Introduction

A prognosis in leukemia during post-remission therapy is very difficult because the number of leukemia cells cannot be detected by light microscopy during this period [1]. Instead of the diagnosis by light microscopy, minimal residual disease (MRD) monitoring is of growing importance for risk stratification and the early detection of relapse in leukemia. For MRD monitoring, several different techniques have been introduced, such as quantitative polymerase chain reaction (PCR), flow cytometry, and cytogenetic measurements [2]. The most sensitive technique appears to be quantitative PCR. Thus, the molecular monitoring of MRD by quantitative PCR was shown to have great potentials to identify patients groups at high risk of relapse and therefore provides a window for therapeutic intervention [3].

Common targets for MRD monitoring by quantitative PCR include leukemia type-specific fusion gene markers such as *BCR/ABL* in chronic myeloid leukemia (CML) [4], *AML1/ETO*, and *PML/RARα* in acute myeloid leukemia (AML) [5].

However, more than 50% of all AML samples lack one of these specific fusion genes. Hence, it is crucial to find more universal molecular targets for MRD detection and quantification in leukemia. The Wilms' tumor gene (WT1) has been reported to be a pan-leukemia marker. Because WT1 mRNA is aberrantly expressed in patients with various types of leukemia [6, 7], the molecular monitoring of this gene may have potentials to elucidate accurately and reproducibly the behaviors of leukemia cells in patients.

The WT1 gene encodes 10 exons and generates a 3 kb mRNA [8, 9]. WT1 mRNA encodes four zinc-finger transcription factors affecting the expression of several growth factors and their corresponding receptors [3]. Although several modifications can occur during mRNA transcription, two predominant alternative splicing regions exist. The first alternative splicing introduces exon 5, encoding 17 amino acids (17AA), just proximal to the first of the four zinc fingers. The second one results in an insertion of three amino acids, lysine, threonine, and serine (KTS) between the third and fourth zinc fingers, the 3′ end of the exon 9 [8, 9]. The alternative splicing of these two sites triggers four different protein isoforms designated as (+/+), (+/–), (–/+), and (–/–), representing the presence or absence of exon 5 and KTS insert [9]. It is yet unclear which isoform affects the kinetics of leukemia [3]; therefore, all of the four WT1 mRNA isoforms should be quantified.

WT1 mRNA quantification using real-time RT-PCR has already been used for MRD monitoring because of its high sensitivity. However, the method is based on the 2 step RT-PCR and furthermore, the quantification of the GAPDH in the separated assay is required. Therefore, the method requires a lot of time and hands. Moreover, the cross

contamination would threatens to affect to the reliability of the assay. In contrast, two novel approaches, which are able to quantify target DNA, have a potential to overcome these shortcomings. The one is the loop-mediated isothermal amplification (LAMP) [10] that allows DNA amplification with high specificity, sensitivity, and rapidity under isothermal conditions ranging from 60–65ºC in a short time (15–60 min) [11, 12]. The LAMP is also useful for RNA amplification with only adding the reverse transcriptase to LAMP mixture [13, 14]. The other is the alternately binding quenching probe competitive PCR (ABC-PCR) [15] that enables us to quantify target of the interest despite the existence of the PCR amplification inhibitors. The method is based on the competitive PCR and the target DNA/RNA is quantified by use of a simple fluorometer at the end of the reaction. Therefore, the ABC-PCR can be performed simply. Moreover, the method is possibly able to utilize the roughly extracted DNA/RNA samples because the method has robustness to several PCR amplification inhibitors.

In this study, the two methods for the simple and rapid WT1 mRNA quantitation were established as follows: First, I designed a LAMP primer set, which amplifies a target sequence in WT1 mRNA for MRD monitoring. The primer/probe set for the ABC RT-PCR was also designed. Second, I assessed the specificity, rapidity, and sensitivity of the RT-LAMP assay in comparison with those of RT-PCR [16]. Also, the MRD monitorings of two patients with acute leukemias were performed using ABC RT-PCR. Finally, I discussed the advantages of the two methods for MRD monitoring in comparison with real-time RT-PCR.

2.2. Materials and Methods

2.2.1. Oligonucleotides

The sequences of primers and AB-Probe are listed in Table 2.1. All the primers were purchased from Tsukuba Oligo Services Co., Ltd., Ibaraki, Japan. The AB-Probe labeled at a 5′ end with TAMRA and at a 3′ end with BODIPY FL was purchased from J-Bio 21 Corp., Ibaraki, Japan. The specificity of the primers and AB-Probe were verified by a database search using BLAST from the DNA data bank of Japan (DDBJ).

2.2.2. Sample

The NIH Mammalian Gene Collection (MGC) Clone was purchased from Invitrogen, CA, USA and used in this study. The MGC Clone contains the WT1 cDNA isoform B (GenBank accession no. BC032861) in the pCMV•SPORT6 plasmid vector transformed in T1-phage-resistant *Escherichia coli*. The *E. coli* was cultured in LB/ampicillin liquid medium at 37ºC for 16 hours. Then the plasmid DNA was isolated from 1.5 mL of cultured cells using the QIAprep Spin Miniprep Kit (Qiagen, Hilden, Germany). PCR was performed using the plasmid DNA. The primers for this assay, F-SP6-WT1 and R-WT1, were designed between the two alternative splicing regions (17AA and KTS), and the SP6 promoter was attached to the forward primer for the *in vitro* transcription. The primers were purchased from Hokkaido System Science Co., Ltd., Hokkaido, Japan. The final concentrations of the reagents in 50 μL of PCR reaction mixture were 10 mM Tris-HCl (pH 8.3), 50 mM KCl, 1.5 mM $MgCl_2$, 0.5 μM of each primer, 0.2 mM of each dNTP, 1.25 units of TaKaRa *Taq* HS DNA polymerase (TaKaRa Bio, Shiga, Japan), and 1 μL of template DNA. The thermal profiles for PCR were as follows: 94ºC for 5 min, followed by 30 cycles of 94ºC for 30 s, 52ºC for 30 s and 72ºC for 60 s, and a final extension cycle at 72ºC for 2 min. The PCR product was purified using Microcon

YM-50 (Millipore, MA, USA).

Table 2.1. Oligonucleotide primers and probe for quantifying WT1 mRNA

Name	*Position	Sequences (5'-3')	Used for	Reference
Primer				
F-SP6-WT1		att tag gtg aca cta tag aat aca cga gag cga taa cca cac aa	standard RNA construction	this study
R-WT1		gat cag cta tgg ctc ttc tta c	standard RNA construction	this study
F3-WT1	688-707	gga gcc caa tac aga atg ca	RT-LAMP	this study
B3-WT1	919-939	acg aga aaa cct tcg ttc aca	RT-LAMP/ABC RT-PCR	this study
FIP-WT1	F2: 713-731 F1: 793-811	tga agg ggc gtt tct cac tac ggt gtc ttc aga ggc at	RT-LAMP	this study
BIP-WT1	B1: 817-837 B2: 895-916	gct tac cca ggc tgc aat aag cct tga agt cac act ggt atg g	RT-LAMP	this study
FLP-WT1	770-791	gtc tca gat gcc gac cgt aca a	RT-LAMP	this study
BLP-WT1	862-883	cag atg cac agc agg aag cac a	RT-LAMP	this study
Fabc-WT1	825-850	agg ctg caa taa gag ata ttt taa gc	ABC RT-PCR	this study
Probe				
ABP-WT1	859-886	(TAMRA)-cag tgt gct tcc tgc tgt gca tct gta a-(BODIPY-FL)	ABC RT-PCR	this study

* Genome position according to the Homo Sapiens WT1 mRNA complete cds (GenBank accession No. BC032861)

The concentration of the product was measured using Agilent 2100 Bioanalyzer (Agilent Technology, CA, USA) and then prepared as 1.0 μg/μL. WT1 mRNA was transcribed *in vitro* from 1 μL of the PCR product using Riboprobe® System-SP6 (Promega, WI, USA) and the phenol/chloroform extraction was performed on the resulting liquid. After measuring the concentration of WT1 mRNA using Agilent 2100 Bioanalyzer (Agilent Technology), the mRNA was stored at −80ºC until use.

2.2.3. Real-time turbidimetry RT-LAMP

Real-time turbidimetry RT-LAMP was performed using the spectrophotometric analysis with the Loopamp real-time turbidimeter LA-200 (Teramecs, Kyoyo, Japan). This apparatus is for the real-time monitoring of the increase in turbidity derived from magnesium pyrophosphate, which is a byproduct of LAMP. The reaction mixture (25 μL) consists of 20 mM Tris-HCl (pH 8.8), 10 mM KCl, 10 mM $(NH_4)_2SO_4$, 8 mM $MgSO_4$, 1 M betaine (Kanto Chemical, Tokyo, Japan), 0.4 mM dNTP Mix, 0.2 μM each of F3-WT1 and B3-WT1, 0.8 μM each of inner primer FIP-WT1 and BIP-WT1, 0.8 μM each of FLP-WT1 and BLP-WT1, 8 units of *Bst* DNA polymerase (New England BioLabs, MA, USA), 0.5 units of Avian myeloblastosis virus (AMV) Reverse Transcriptase XL (TaKaRa Bio), and 1 μL of template mRNA. The template mRNA was diluted with DEPC-treated water to prepare serial 10-fold dilutions of template mRNA ranging from 6.8×10 to 6.8×10^9 copies, and then added into the mixture. The no-template control contained water instead of the template, and the no-reverse transcriptase (RTase) control, in which 10^5 copies of template mRNA was added, contained water instead of the RTase. The mixture was incubated at 62ºC for 60 min. Real-time RT-LAMP was performed in triplicate for each template mRNA.

2.2.4. Real-time RT-PCR

Real-time RT-PCR was performed using One Step SYBR® PrimeScript® RT-PCR Kit II (TaKaRa Bio) and LightCycler® ST300 (Roche Diagnostics, Basel, Switzerland). The reaction mixture (20 μL) contained 0.4 μM each of F3-WT1 and B3-WT1, 10 μL of 1 × One Step SYBR® RT-PCR buffer 4, and 0.8 μL of PrimeScript® one step Enzyme Mix 2. The thermal cycling profile consisted of a 10-min reverse transcription step at 42ºC, 10 s of RTase inactivation at 95ºC, followed by 40 cycles of PCR consisting of denaturing for 5 s at 95ºC, annealing for 10 s at 55ºC, and extension for 15 s at 72ºC. Real-time RT-PCR was performed in triplicate for each template mRNA. Results were analyzed using LightCycler software version 3.5 (Roche Diagnostics).

2.2.5. ABC RT-PCR

ABC RT-PCR was carried out according to the description by Tani [17]. In detail, the PCR mixture (25 μL) contained 20 U SuperScript® III RTase (Invitrogen), 1× TITANIUM Taq DNA polymerase (Clontech, Shiga, Japan), 1.0 μL of 1 × TITANIUM buffer, 200 μM of each dNTPs mix (TaKaRa Bio, Shiga, Japan), 0.12 μM of ABP-WT1, 0.5 μM of Fabc-WT1, 0.15 μM of B3-WT1, 10^3 copies of competitor RNA, and 1 μL of template mRNA. The PCR conditions were as follows: reverse transcription at 42ºC for 30 min, initial denaturation at 94ºC for 3 min; 50 cycles of denaturation at 94ºC for 20 s, annealing at 61ºC for 20 s, and extension at 72ºC for 20 s; and a final extension at 72ºC for 2 min. The PCR was performed using the Veriti® 96-well (Applied Biosystems, CA, USA) in triplicate for each template mRNA, and the no-temlate control (NTC) contained DEPC treated water instead of the target and competitor RNA. After the PCR amplification, the fluorescence intensity of each aliquot was measured using ABI 7500 (Applied Biosystems) at 95ºC and 55ºC. The fluorescence raw data was analyzed

according to the previous study [15]. The fluorescence intensity of the green dye (G_{95}) and the red dye (R_{95}) at 95ºC represented the intensities before hybridization, whereas those of the green dye (G_{55}) and the red dye (R_{55}) at 55ºC represented the intensities after hybridization. In order to normalize for non-PCR-related fluorescence intensity fluctuations occurring between reaction tubes, G_{55} and R_{55} were then divided by G_{95} and R_{95}, respectively. The measured fluorescence intensities of the green dye (G_{55}/G_{95}) and the red dye (R_{55}/R_{95}) are the sum of the fluorescence intensities from the unbound probe (G_U or R_U), the hybridized probe with the target (G_T or R_T), and the hybridized probe with the competitor (G_C or R_C). The standard curves were obtained by fitting the relationship between $[(G_{55}/G_{95}) - G_U]/[R_U - (R_{55}/R_{95})]$ and starting quantity of the target to a sigmoid curve.

2.3. Results

2.3.1. Primer design

Primers and probe were designed on the basis of the sequences between the 17AA and KTS regions to establish RT-LAMP assay and ABC RT-PCR that can detect all of the four WT1 mRNA isoforms (Figure 2.1). The nucleotide sequence of WT1 cDNA (GenBank accession no. BC032861) was used for the primer/probe design. A set of six primers comprising two outer (F3-WT1 and B3-WT1), two inner (FIP-WT1 and BIP-WT1), and two loop primers (FLP-WT and BLP-WT1) was designed using PrimerEXplorer V3 (URL: http://primerexplorer.jp/e/). FIP-WT1 consists of the complementary sequence of F1-WT1 and the sequence of F2-WT1. BIP-WT1 consists of the sequence of B1-WT1 and the complementary sequence of B2-WT1. F3-WT1 and B3-WT1 were located outside F2-WT1 and B2-WT1, respectively. A pair of loop primers (FLP-WT1 and BLP-WT1) was used to shorten the reaction time. FLP-WT1 was located between the 3' end of the F2-WT1 region and the 5' end of the F1-WT1 region. BLP-WT1 was located between the 3' end of the B1-WT1 region and the 5' end of the B2-WT1 region. Figure 2.2 shows the locations of the primers for RT-LAMP along with the alignment of the WT1 cDNA sequence. Furthermore, a database search using BLAST from the DNA Data Bank of Japan (DDBJ) showed that all the primers and the probe were specific only to WT1 mRNA.

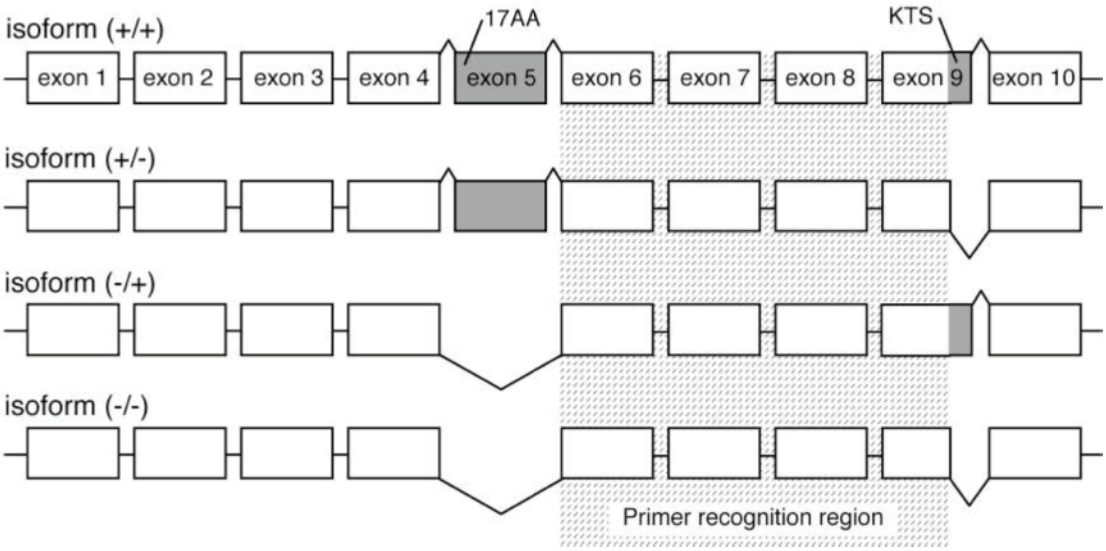

Figure 2.1. A schematic of WT1 mRNA. 17AA and KTS regions, at which alternative splicing can occur, are in gray. Alternative splicing generates four isoforms designated as (+/+), (+/–), (–/+), and (–/–). The dotted area indicates the common region of the four isoforms. The primer recognition region is located in the dotted area.

Figure 2.2. A schematic showing the location of primers for RT-LAMP. The DNA sequences of the primer recognition regions are shadowed, and the arrow indicates the direction of the primer extension. The *Hin*fI target site is shown in a box. The sequence was obtained from GenBank with accession number BC032861; the genome position was 688–939.

2.3.2. RT-LAMP Quantification

Real-time RT-LAMP was performed to determine the detection limit, quantification limit, and dynamic range of this assay. The template mRNA was prepared as serial 10-fold dilutions ranging from 6.8 × 10 to 6.8 × 10^9 copies and then added into the RT-LAMP mixture. Each turbidity curve increases with the increase in the copy number of the template mRNA. Moreover, all turbidity curves exceed the threshold time (*Tt*) within approximately 30 min (Figure 2.3.A). *Tt* is defined as the time at which the turbidity exceeds a certain value. In this study, I determined that the value to be 0.03. Even in the case of 6.8 × 10 copies, the template mRNA can be detected by RT-LAMP (Figure 2.3.A); therefore, the detection limit was determined to be 6.8 × 10 copies per reaction tube.

The standard curve was plotted with the log copy numbers of the initial template mRNA versus *Tt*. Figure 2.3.B shows the linear relationship between the logarithmic copy numbers of the initial template mRNA and the *Tt* with a correlation coefficient of R^2 > 0.994 ranging from 6.8 × 10 to 6.8 × 10^9 copies. Consequently, the lower quantification limit and the dynamic range were determined to be 6.8 × 10 copies and 9 orders of magnitude, respectively.

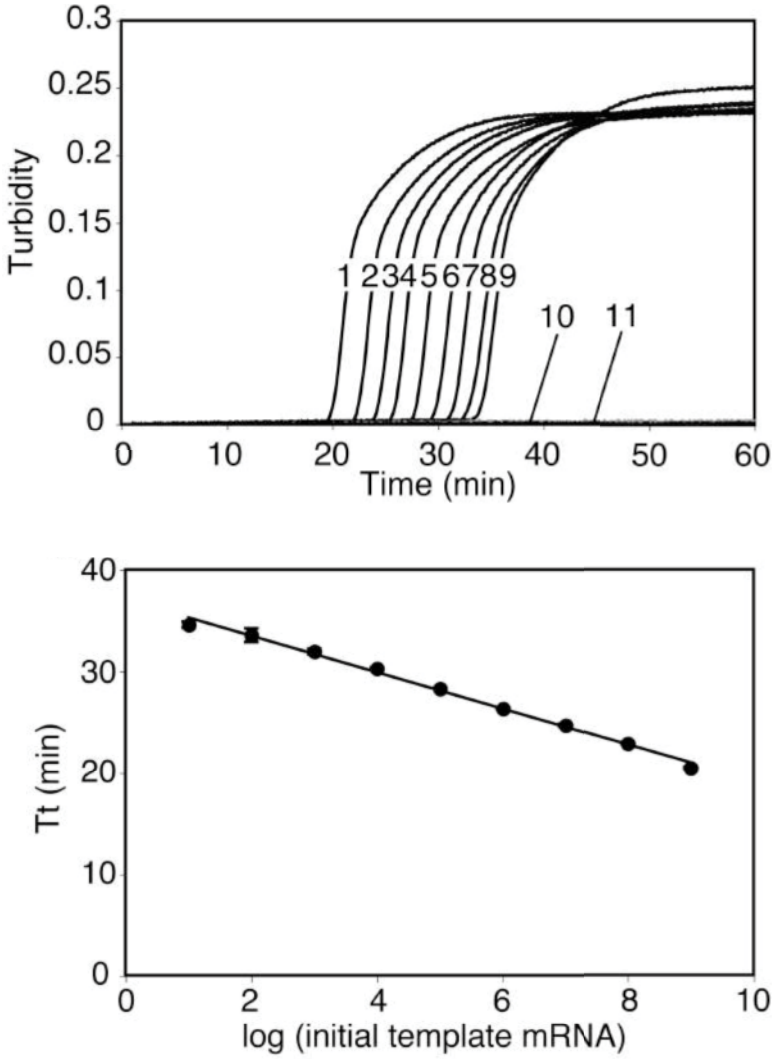

Figure 2.3. Real-time RT-LAMP with serial 10-fold dilutions of WT1 mRNA. A: Turbidity profiles. Serial 10-fold dilutions: (1) 6.8×10^9, (2) 6.8×10^8, (3) 6.8×10^7, (4) 6.8×10^6, (5) 6.8×10^5, (6) 6.8×10^4, (7) 6.8×10^3, (8) 6.8×10^2, and (9) 6.8×10 copies of WT1 mRNA were amplified using RT-LAMP in triplicate. No turbidities of the no-RTase (10) and the no-template (11) controls were detected. B: Typical standard curve. The standard curve was obtained by fitting the data points linearly. $y = -1.7861x + 37.06$; R^2 was calculated as 0.9945. Data points and cross bars represent the means and standard deviations, respectively.

2.3.3. Accuracy of RT-LAMP

To determine the accuracy of RT-LAMP, 2.5, 25, and 250 fg of WT1 mRNA were mixed with 0.1 ng of total HeLa RNA and quantified using RT-LAMP. Real-time RT-PCR was also applied to the same sample, and the results were compared. The experiments were repeated three times, and the mean number of WT1 mRNA copies and SD for each amount of RNA were calculated. Each amount of WT1 mRNA (2.5, 25, and 250 fg) corresponds to 5.0×10^3, 5.0×10^4, and 5.0×10^5 copies, respectively. Figure 2.4 shows that the results of RT-LAMP strongly correlated with true values and those of real-time RT-PCR. Furthermore, the RSD values for 2.5, 25, and 250 fg in the case of RT-LAMP were 22, 21, and 35 %, while those in the case of real-time RT-PCR were 59, 16, and 23 %, respectively. These results indicate that RT-LAMP can accurately quantify specific mRNA sequences and has an accuracy similar to that of real-time RT-PCR.

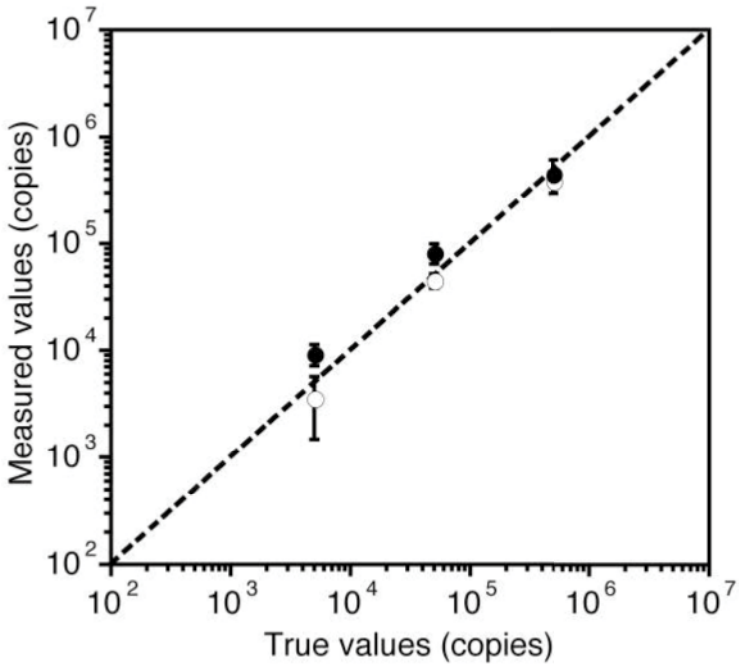

Figure 2.4. Quantification of WT1 mRNA in crude samples. WT1 mRNA was mixed with 0.1 ng of total HeLa RNA and quantified using RT-LAMP (solid circles) and real-time RT-PCR (open circles) in triplicate. All experiments were performed three times. The dashed line corresponds to the true values. The error bars represent the standard deviation of three independent experiments.

2.3.4 Monitoring of WT1 mRNA expression level by ABC RT-PCR

I constructed a standard curve for quantifying the expression level of WT1 mRNA. Various amounts of the WT1 mRNA as target, ranging form 10–10^5 copies in the presence of 10^3 copies of competitor RNA, were prepared. The RNA mixtures were amplified by RT-PCR, and then the florescence intensity of each aliquot was measured. After measuring the fluorescence intensity, $[(G_{55}/G_{95}) - G_u]/[R_u - (R_{55}/R_{95})]$ was plotted against the copy number of the initial quantity of WT1 mRNA (Figure 2.5). The results showed that the $[(G_{55}/G_{95}) - G_u]/[R_u - (R_{55}/R_{95})]$ values obtained from triplicate samples showed good fitting to a sigmoid curve with a correlation coefficient (R^2) of 0.997. The standard deviation (SD) of triplicate determinations was less than 0.079 for 10 to 10^5 copies.

Next, total RNA was extracted from the bone marrow samples of 2 patients with acute leukemia (the one is acute promyelocytic leukemia, the other is refractory acute myeloid leukemia) attending the University of Yamanashi Hospital (Chuo, Yamanashi, Japan). Institutional Ethics Committee approval was obtained at the institution and written informed consent was obtained from each patient. The bone marrow samples were obtained during the follow-up of each patient. The WT1 mRNA expression level of each patient was quantified using ABC RT-PCR, then the quantified values were represented as the expression level per 1.0 μg total RNA. The expression level of WT1 mRNA closely linked to the conditions of each patient (Figure 2.6 A, B).

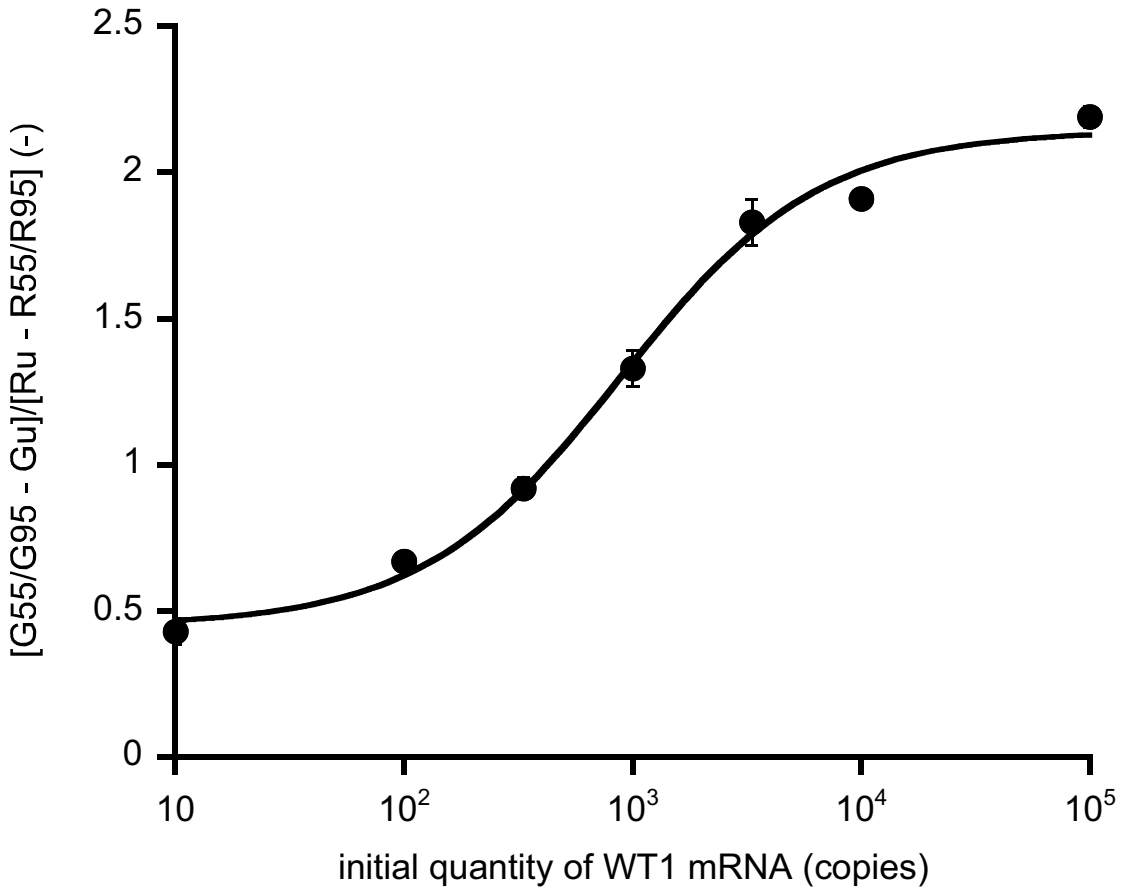

Figure 2.5. Typical standard curve. A fixed amount of the competitor (10^3 copies) was coamplified with various amounts of the target WT1 mRNA (10, 10^2, 3.3×10^2, 10^3, 3.3×10^3, 10^4, and 10^5 copies) in triplicate samples. G_U and R_U were measured from the fluorescence intensities of the green and the red dyes of the NTC, respectively. The standard curve was obtained by fitting the data points to a sigmoid curve. $y = -1468.7/[888.7 + x] + 2.14$; the correlation coefficient (R^2) was calculated to be 0.997. The error bars represent the SD of triplicate determinations per dilution.

B

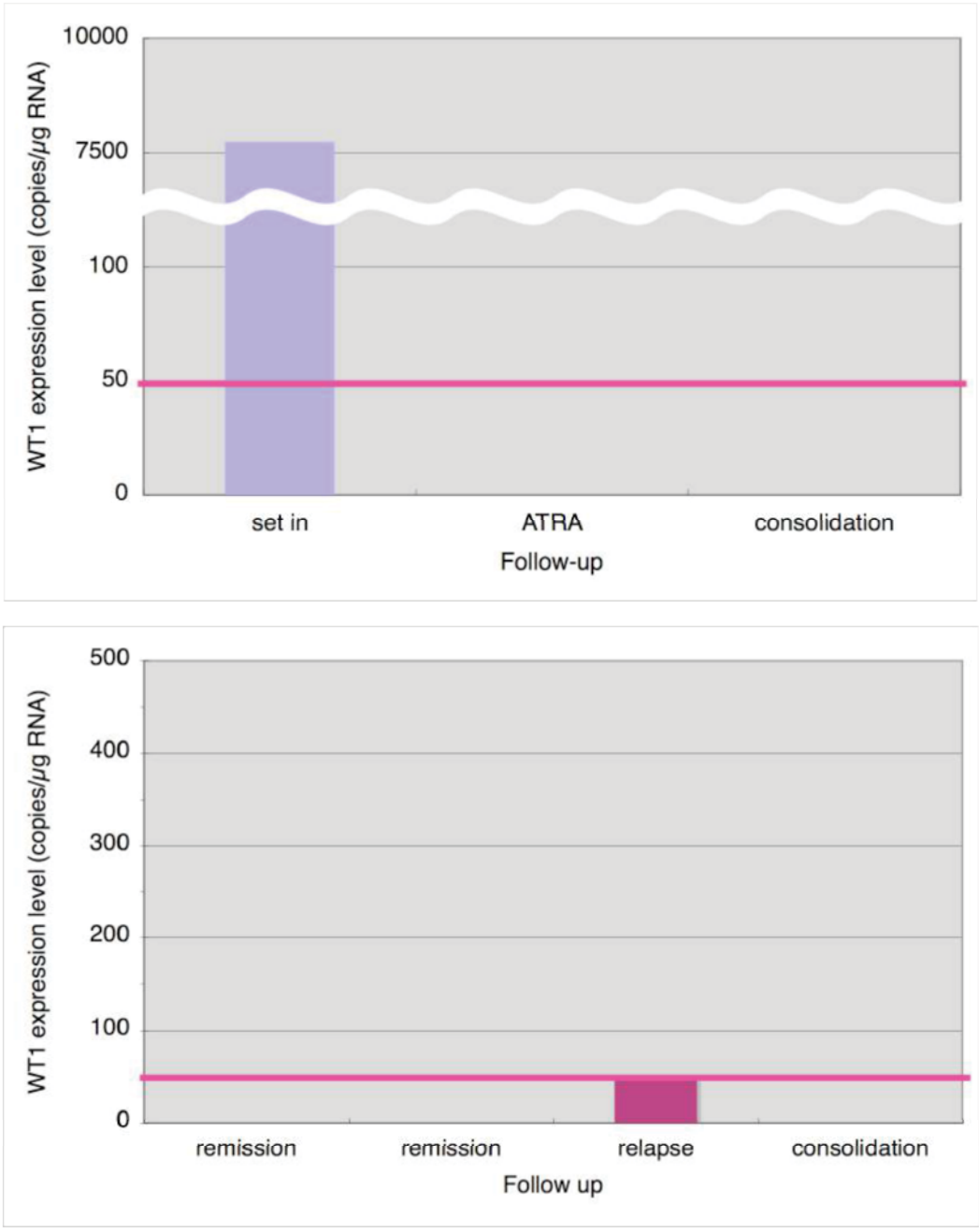

Figure 2.6. Transition of WT1 expression level in patients with acute leukemias using ABC RT-PCR. Fuchsia line indicates the lower quantitation limit of the conventional real-time RT-PCR. ATRA, all-trans retinoic acid therapy; and consolidation, consolidation therapy. A: Patient with acute promyelocytic leukemia, B: Patient with refractory acute myeloid leukemia.

2.4. Discussion

A universal leukemia marker is crucial for monitoring MRD comprehensively in various types of leukemia. Several fusion genes have been raised as candidate markers for MRD monitoring; however, these genes are expressed in specific types of leukemia. Therefore, fusion genes are not appropriate as universal markers. In contrast, WT1 mRNA can be used as such a universal marker because this gene is highly expressed in various types of leukemia [18]. In this study, the quantification of WT1 mRNA using two methods is described. The one is RT-LAMP, which can be performed specifically, rapidly, and simply, and the other is ABC RT-PCR, which can be performed simply with high flexibility to the samples.

All the primers for RT-LAMP and ABC RT-PCR were designed so that all the four WT1 mRNA isoforms can be quantified. This is because various WT1 mRNA isoforms are overexpressed in leukemia patients and it is yet unclear which isoform affects leukemia kinetics [3]. The result of a database search with BLAST strongly suggests that the designed primer set binds to target sequences specifically.

RT-LAMP is completed within 30 min in this study (Figure 2.3.A). Real-time RT-PCR usually requires 2–3 hours to finish; therefore, RT-LAMP is a more rapid assay than PCR. The rapid quantification of WT1 mRNA can be used to effectively monitor MRD and provide frequent feedback concerning the treatment. Moreover, MRD monitoring can be carried out simply by RT-LAMP because cDNA synthesis and follow-up amplification can be achieved in a single tube with only basic equipment such as a water bath or heated block [13, 14]. Because of its rapidity and simplicity, RT-LAMP has the potential to be used for bedside MRD monitoring.

The lower limits of detection and quantification are both determined as 10 copies in a reaction tube. The dynamic range of this assay was also estimated to be 9 orders of magnitude (Figure 2.3.A, B). The quantification of WT1 mRNA expression level using real-time RT-PCR has been reported [16], in which the lower limits of detection and quantification and dynamic range of the assay were determined to be 10 copies per reaction and 7 orders in magnitude, respectively. Therefore, the lower quantitative limit of RT-LAMP is the same as that of real-time RT-PCR, and RT-LAMP is better than real-time RT-PCR in terms of the dynamic range. Moreover, the accuracy of RT-LAMP was compared with that of real-time RT-PCR. In this experiment, 2.5, 25, and 250 fg of WT1 mRNA were quantified using both RT-LAMP and real-time RT-PCR in the presence of 0.1 ng of total HeLa RNA, which was used as a background RNA. Results showed that RT-LAMP was able to specifically quantify WT1 mRNA in crude samples because the amount of total HeLa RNA was sufficient against those of WT1 mRNA, and the accuracy of RT-LAMP was similar to that of real-time RT-PCR (Figure 2.4). These results suggest that RT-LAMP has an outstanding lower limit of quantification, wide dynamic range, and sufficient accuracy for quantifying target mRNA.

The expression level of WT1 mRNA in patients with acute leukemia closely linked to the therapeutic events (Figure 2.6 A, B). However, in the remission or the consolidation therapy events, WT1 mRNA could not be quantified by use of the ABC RT-PCR because the fluorescence intensities of the samples were out of range of the standard curves. The bone marrow samples use in this study was originally collected for other purposes. Therefore, the samples were stored without any RNA stabilizing treatments for approximately a year. This might lead to the degradation of RNAs in the samples. Despite the fact, the MRD monitoring managed to be performed using ABC RT-PCR.

Two reasons may be taken into consideration. First, the RNA samples were derived from bone marrow. The WT1 mRNA expression level in bone marrow is generally higher than those in peripheral blood [19]. Therefore, RNA compartment could be avoided from the complete degradation. Second, the ABC RT-PCR has the flexibility to the conditions of the target. The ABC assay is able to accurately quantify target nucleic acid even in the existence of the PCR amplification inhibitors [15]. Therefore, the WT1 expression level of so-called old samples might be quantified using ABC RT-PCR.

2.5. Conclusion

In summary, the pan-leukemia marker WT1 mRNA can be quantified using two novel developed methods. The RT-LAMP can be performed specifically, rapidly, and simply. Moreover, the quantitative range of RT-LAMP was found to be the same as that of real-time RT-PCR. The ABC RT-PCR has a potential to monitor the MRD of the acute leukemia. Several methods for the MRD monitoring such as the methods developed in this study would be contribute to widening the selection of the method on demand.

References

1. Mortuza F. Y., Papaioannov M., Moreira I. M., et al. Minimal residual disease tests provide an independent predictor of clinical outcome in adult acute lymphoblastic leukemia. *J. Clin. Oncol.* 2002; **20:** 1094-104.
2. Sperr W. R., Mitterbauer M., Mitterbeuer G., et al. Quantification of minimal residual disease in acute myeloid leukemia by tryptase monitoring identifies a group of patients with a high risk of relapse. *Clin. Cancer Res.* 2005; **11:** 6536-43.
3. Weisser M., Kern W., Rauhut S., et al. Prognostic impact of RT-PCR based quantification of WT1 gene expression during MRD monitoring of acute myeloid leukemia. *Leukemia* 2005; **19:** 1416-23.
4. Winn-Deen E. S., Helton B., Atta R. V., et al. Development of an integrated assay for detection of *BCR-ABL* RNA. *Clin. Chem.* 2007; **53:** 1593-600.
5. Inoue K., Sugiyama H., Ogawa H., et al. WT1 as a new prognostic factor and a new marker for the detection of minimal residual disease in acute leukemia. *Blood* 1994; **84:** 3071-9.
6. Schultz K. R., Pullen D. J., Sather H. N., et al. Risk- and response-based classification of childhood B-precursor acute lymphoblastic leukemia: a combined analysis of prognostic markers from the Pediatric Oncology Group (POG) and Children's Cancer Group (CCG). *Blood* 2007; **109:** 926-35.
7. Østergaard M., Olesen L. H., Hasle H., Kjeldsen E., and Hokland P. WT1 gene expression: an excellent tool for monitoring minimal residual disease in 70% of acute myeloid leukaemia patients – results from a single-centre study. *Br. J. Haematol.* 2004; **125:** 590-600.
8. Wagner K. J. and Roberts S. G. E. Transcriptional regulation by the Wilms' tumour suppressor protein WT1. *Biochem. Soc. Trans.* 2004; **32:** 932-5.

9. Yang L., Han Y., Saurez F., and Minden M. D. A tumor suppressor and oncogene: the WT1 story. *Leukemia* 2007; **21:** 868-76.

10. Notomi T., Okayama H., Masubuchi H., et al. Loop-mediated isothermal amplification of DNA. *Nucleic Acids Res.* 2000; **28:** e63.

11. Mori Y., Kitao M., Tomita N., and Notomi T. Real-time turbidimetry of LAMP reaction for quantifying template DNA. *Biochem. Biophys. Meth.* 2004; **59:** 145-57.

12. Aoi Y., Hosogai M., and Tsuneda S. Real-time quantitative LAMP (loop-mediated isothermal amplification of DNA) as a simple method for monitoring ammonia-oxidizing bacteria. *J. Biotech.* 2006; **125:** 484-91.

13. Toriniwa H. and Komiya T. Rapid detection and quantification of Japanese encephalitis virus by real-time reverse transcription loop-mediated isothermal amplification. *Microbiol. Immunol.* 2006; **50:** 379-87.

14. Parida M., Posadas G., Inoue S., Hasebe F., Morita K. Real-time reverse transcription loop-mediated isothermal amplification for rapid detection of West Nile virus. *J. Clin. Microbiol.* 2004; **42:** 257-63.

15. Tani H., Kanagawa T., Kurata S., Teramura T., Nakamura K., Tsuneda S., and Noda N. Quantitative method for specific nucleic acid sequences using competitive polymerase chain reaction with an alternately binding probe. *Anal. Chem.* 2007; **79:** 974-9.

16. Kreuzer K. A., Saborowski A., Lupberger J., et al. Fluorescent 5'-exonuclease assay for the absolute quantification of Wilms' tumor gene (WT1) mRNA: implications for monitoring human leukaemias. *Br. J. Haematol.* 2001; **114:** 313-8.

17. Tani H. Development of quantitative method for specific nucleic acid sequences using fluorescence quenching phenomenon. PhD thesis 2008; Waseda University,

Tokyo, Japan.

18. Ogawa H., Tamaki H., Ikegame K., et al. The usefulness of monitoring WT1 gene transcripts for the prediction and management of relapse following allogeneic stem cell transplantation in acute type leukemia. *Blood* 2003; **101:** 1698-704.
19. Collini D., Gottardi E., De Micheli D., et al. Quantitative assessment of WT1 expression by real time quantitative PCR may be a useful tool for monitoring minimal residual disease in acute leukemia patients. *Leukemia* 2002; **16:** 2115-21.

Chapter 3

Simple, cost-effective, and accurate JAK2 allele burden quantification for the myeloproliferative neoplasms

Chapter 3

Simple, cost-effective, and accurate JAK2 allele burden quantification for the myeloproliferative neoplasms

3

3.1. Introduction

Classical myeloproliferative neoplasms (MPNs), essential thrombocythemia (ET), polycythemia vera (PV), and primary myelofibrosis (PMF) have a common somatic point mutation, JAK2V617F [1-3]. JAK2V617F is the alteration of the guanine base (G) to the thymine base (T) in the 73rd base of exon 14. This mutation triggers the homeostatic activation of the JAK2 protein [4]. JAK2V617F is found in 45% of ET patients, 95% of PV patients, and ~50% of PMF patients [5]. The discovery of this gene mutation has markedly improved the diagnosis of MPNs. The detection of JAK2V617F is now one of the major criteria for the diagnosis of MPNs [6]. However, the detection of JAK2V617F would not be sufficient because heterozygous JAK2V617F cells, homozygous JAK2V617F cells, and wild type cells are randomly and simultaneously detected in a single MPNs patient [7]. Therefore, the quantification of the ratio of the copy number of the JAK2V617F allele to the total copy number of JAK2 alleles (JAK2 allele burden) would be required for the assessment of the size of a JAK2V617F-positive clone. A study using transgenic mice expressing various JAK2 allele burdens showed intriguing results [8]. In that study, mice with low JAK2 allele

burdens showed an ET-like phenotype, whereas mice with higher JAK2 allele burdens showed a PV-like phenotype [8]. Furthermore, quantification of JAK2 allele burden may also be important in the follow-up of patients treated with soon-to-be-available JAK2 inhibitors [9, 10].

Several methods for detecting and/or quantifying JAK2 allele burden have been developed to date, such as melting peak analysis [11] and TaqMan allele-specific quantitative PCR (TaqMan AS-qPCR) [12]. However, these methods have both advantages and disadvantages. The former method can be performed simply to detect JAK2V617F, but cannot quantify JAK2 allele burden. The latter is a highly sensitive (0.1–3%) quantitative method, but requires complicated operations and expensive equipment and reagents [13].

Here, we propose alternately binding probe competitive PCR (ABC-PCR) as a simple, cost-effective, and accurate method of quantifying JAK2 allele burden [14]. ABC-PCR was originally established for the accurate quantification of DNA in samples that contain PCR inhibitors [14, 15]. The method involves the combined use of competitive PCR and a sequence-specific fluorescent probe named an alternately binding probe (AB-Probe). In the case of the quantification of JAK2 allele burden by ABC-PCR, the target JAK2 wild type and mutant type are competitively amplified in a single reaction tube using the same primer set in the presence of the AB-Probe, and then fluorescence intensity is measured at the end point of the PCR. The AB-Probe is labeled at the 5′ end with a red dye (6-carboxytetramethylrhodamine; TAMRA) and at the 3′ end with a green dye (BODIPY FL). The fluorescent dyes are notably quenched by an electron transfer to a guanine base at a particular position [16]. JAK2V617F is an alteration of G

(wild type) to T (mutant type); therefore, fluorescence intensity decreases as the amount of the JAK2 wild type in the target increases. Thus, green fluorescence intensity is in proportion to target JAK2 allele burden (Figure 3.1). Red fluorescence intensity is used for normalizing the aliquot and checking the PCR amplification products. Thus, JAK2 allele burden can be directly quantified from the fluorescence intensity of the AB-Probe at the end point of the PCR. The use of ABC-PCR has mainly three benefits for the quantification of JAK2 allele burden. First, target JAK2 allele burden can be simply quantified by ABC-PCR. As described above, target JAK2 allele burden can be quantified in a single reaction tube. This can reduce the preparation steps of the assay to half those of other assays because other assays usually require two reactions for each target to quantify target JAK2 allele burden. Second, ABC-PCR markedly reduces running cost. The JAK2 allele burden quantification by ABC-PCR assay can be completed with one reaction for each target. Thus, the amount of reagents used in ABC-PCR can be reduced to half. Finally, ABC-PCR can accurately quantify target JAK2 allele burden. The target JAK2 wild type and mutant type are coamplified in a single reaction tube using the same primer set, and target JAK2 allele burden can be directly quantified from the fluorescence intensity of the AB-Probe without quantifying the copy number of each JAK2 allele. Therefore, ABC-PCR can avoid several intrinsic biases such as the difference in tube-to-tube amplification efficiency. On this basis, we hypothesized that target JAK2 allele burden can be accurately quantified by ABC-PCR.

In this study, we have established the ABC-PCR methodology to quantify JAK2 allele burden as follows. First, primers and an AB-Probe for the assay were designed. Then, the range of target JAK2 allele burdens that can be accurately quantified by ABC-PCR was determined using cell-line-derived DNA. Finally, the JAK2 allele burdens in 14

JAK2V617F-positive patients and 10 healthy controls were quantified by ABC-PCR and TaqMan AS-qPCR and compared.

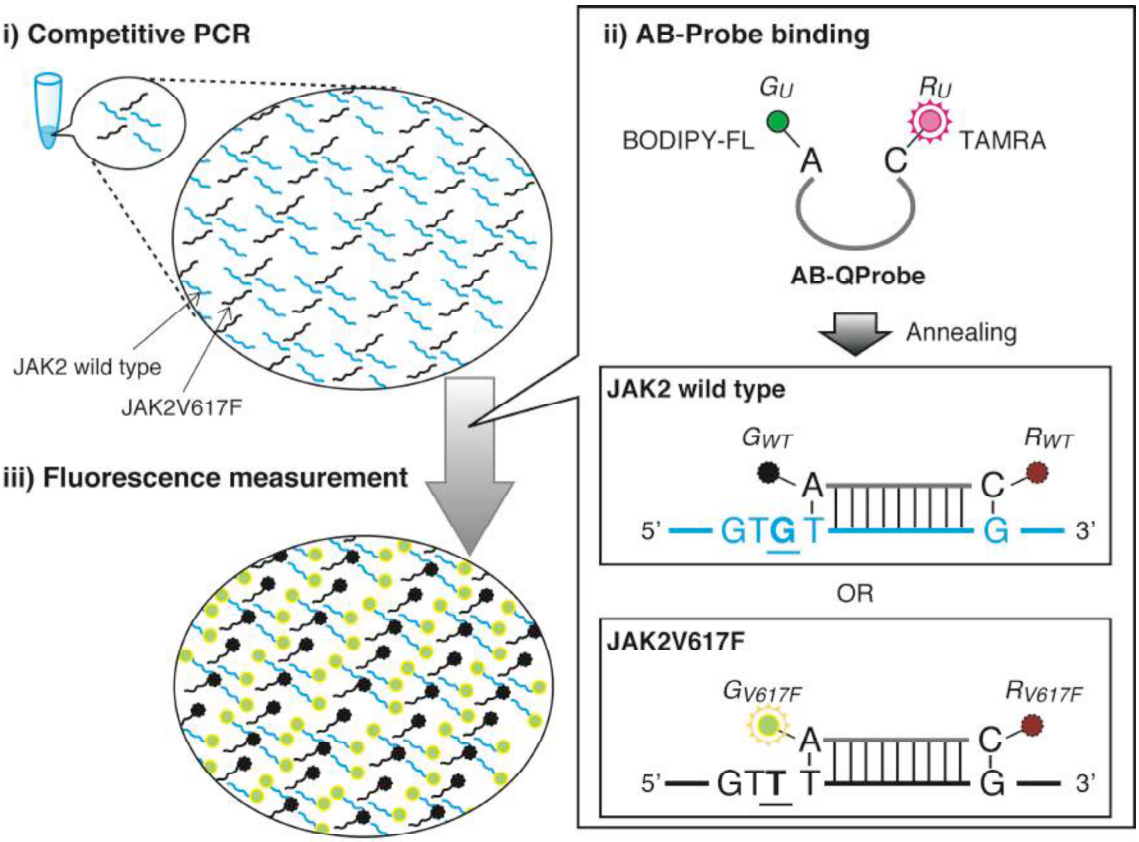

Figure 3.1. Schematic presentation of ABC-PCR assay for quantifying JAK2 allele burden. The blue wavy lines indicate the JAK2 wild-type allele, and the black wavy lines indicate the JAK2V617F allele. Italic characters represent the fluorescence intensities of the dyes under each condition. The underlined bold G and T are the JAK2V617F mutation points. ABC-PCR is performed as follows: i) Competitive amplification of the JAK2 wild type and JAK2V617F sequence using the same primer set. The target allele burden does not change before and after the amplification. ii) The AB-Probe binds to both the JAK2 wild type and JAK2V617F sequence with the same efficiency, and the green fluorescence markedly quenches when the probe binds to the JAK2 wild type. The red fluorescence quenches when the probe binds to both JAK2 alleles, indicating the ratio of the amount of the unbound probe to that of the hybridized probe. iii) The green fluorescence intensity of the AB-Probe reflects the target allele burden.

3.2. Materials and Methods

3.2.1. Cell lines

The UT-7 cell line, which has homozygous JAK2 wild-type alleles, and the HEL cell line, which has homozygous JAK2V617F alleles, were used in this study. UT-7 cells were cultured in IMDM medium (GIBCO, MD, USA) with 10% fetal calf serum (FCS) (GIBCO), 10 ng/ml erythropoietin (EPO), 100 units/ml penicillin (GIBCO), and 100 μg/ml streptomycin (GIBCO) at 37ºC in 5% CO_2. HEL cells were cultured in RPMI 1640 medium (SIGMA, MO, USA) with 10% FCS (GIBCO), 10 ng/ml EPO, 100 units/ml penicillin (GIBCO), and 100 μg/ml streptomycin (GIBCO) at 37ºC in 5% CO_2. EPO was kindly provided by Kyowa Hakko Kirin, Tokyo, Japan. The medium was changed every 3 days. Each culture was centrifuged at 200 × g for 5 min, and then the supernatant was removed. The cells were resuspended in 2 mL of phosphate-buffered saline (PBS) (GIBCO) and then DNAs were extracted from the UT-7 and HEL cells using a QIAamp DNA Mini kit (Qiagen, Hilden, Germany) in accordance with the manufacturer's instructions. After measuring the concentrations of the extracted DNAs using a NanoDrop 1000 spectrophotometer (Thermo Scientific, DE, USA), the DNAs were stored at −80ºC until use.

3.2.2. Oligonucleotides

The sequences of the primers, AB-Probe, and TaqMan probe used are listed in Table 3.1. The relative positions of the primers and probes are shown in Figure 3.2. All the primers were purchased from Tsukuba Oligo Services Co., Ltd., Ibaraki, Japan. The AB-Probe labeled at the 5′ end with TAMRA and the 3′ end with BODIPY FL was purchased from J-Bio 21 Corp., Ibaraki, Japan. The TaqMan probe was purchased from Applied Biosystems, CA, USA. The specificities of the primers, AB-Probe, and

TaqMan probe were verified by a database search using BLAST from the DNA data bank of Japan (DDBJ).

Table 3.1. Sequence of primers and probes used in this study

Name	Sequence (5'–3')	*Position	Used for	Note	Reference
Primer					
F-JAK2-std	cac ttt gat ctc cat att cca g	54772–54793	Standard sample construction	Forward primer for both JAK2 alleles	**this study
R-JAK2-std	ctg cca taa tct ctt ttg c	55365–55347	Standard sample construction	Reverse primer for both JAK2 alleles	**this study
F-JAK2	atc tat agt cat gct gaa agt agg aga aag	54871–54900	ABC-PCR	Forward primer for both JAK2 alleles	1
FTQ-JAK2	tga tga gca agc ttt ctc ac	55011–55030	TaqMan AS-qPCR	Forward primer for both JAK2 alleles	**this study
FAS-JAK2mt	agc att tgg ttt taa att atg gag tat att	55032–55061	TaqMan AS-qPCR	Forward primer for JAK2 mutant allele	1
R-JAK2	ctg aat agt cct aca gtg ttt tca gtt tca	55234–55205	ABC-PCR/TaqMan AS-qPCR	Reverse primer for both JAK2 alleles	1
Probe					
ABP-JAK2	(TAMRA)-cct gta gtt tta ctt act ctc gtc tcc aca ga-(BODIPY)	55093–55062	ABC-PCR	AB-Probe	**this study
TQ-JAK2	(FAM)-tgt gga gac gag agt aa-(MGB)	55064–55080	TaqMan AS-qPCR	TaqMan Probe	17

* The position is based on the sequence obtained from GenBank Accession No. AL161450.
** The specificities of all the primers and probes designed in this study were validated by a database search using BLAST from the DNA data bank of Japan (DDBJ).

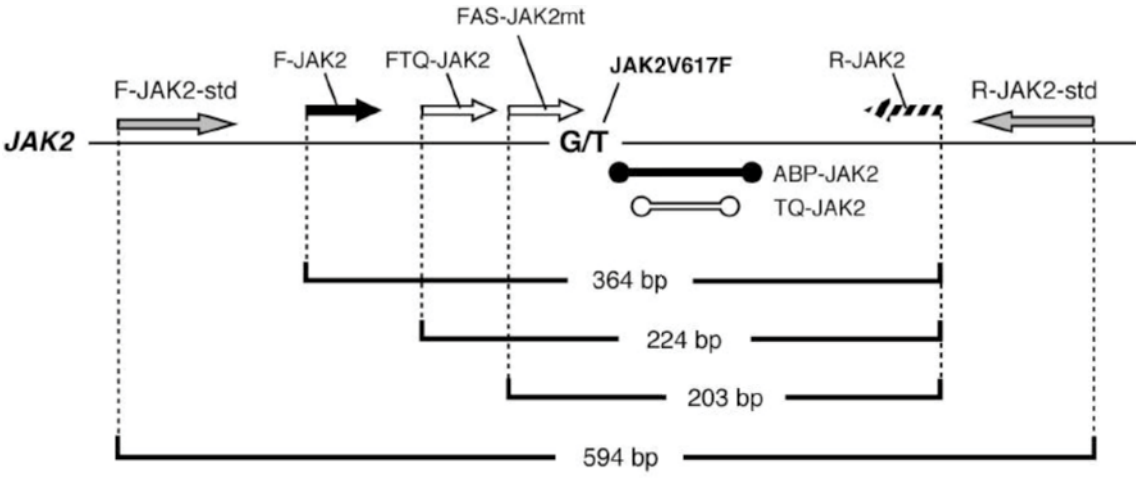

Figure 3.2. Relative positions of primers and probes, and amplicon sizes. Each arrow represents the primers, and the directions of the arrows indicate the direction of the primer extension. Dumbbell-shaped symbols represent the fluorescence-labeled probes. The black symbols are the primer/probe set used for ABC-PCR, the white symbols are the primer/probe sets for TaqMan AS-qPCR. R-JAK2 (striped arrow) is the common reverse primer for ABC-PCR and TaqMan AS-qPCR. The gray arrows are used for the construction of the standard samples.

3.2.3. Preparation of standard samples

The DNAs extracted from the UT-7 and HEL cells were amplified by PCR using a Veriti® 96-well Thermal Cycler (Applied Biosystems, CA, USA) to obtain a 594 bp DNA fragment. The reaction mixture (50 μL) contained 1× TaKaRa Taq HS (TaKaRa Bio, Shiga, Japan), 5.0 μL of 10× PCR buffer, 200 μM each of dNTPs (TaKaRa Bio), 0.5 μM each of F-JAK2-std and R-JAK2-std, and 1 μL of extracted DNA. The PCR conditions were as follows: initial denaturation at 95ºC for 2 min; 30 cycles of denaturation at 95ºC for 30 s, annealing at 58ºC for 30 s, and extension at 72ºC for 40 s; and a final extension at 72ºC for 2 min. Subsequently, the obtained PCR products were purified using a Microcon YM-50 (Millipore, MA, USA). The fragment length and concentration of the purified products were determined using an Agilent 2100 Bioanalyzer (Agilent Technologies, CA, USA). The PCR products obtained from the UT-7 and HEL cells were mixed in different proportions (99%, 90%, 70%, 50%, 30%, 10%, 5%, and 1% JAK2 allele burdens) at a concentration of 10^5 copies/μl and then used as the standard samples for ABC-PCR. Serial 10-fold dilutions of the PCR product from HEL cells at 10–10^6 copies/μl were prepared as the standard samples for use in TaqMan AS-qPCR.

3.2.4. DNA with known JAK2 allele burden

DNA samples with known JAK2 allele burdens were prepared by mixing the DNA from UT-7 and HEL cells. We considered that the JAK2 copy numbers of the two cell lines were different because the UT-7 and HEL cell lines were derived from megakaryoblastic leukemia and erythroleukemia, respectively. Therefore, the JAK2 copy number of each extracted DNA sample was quantified by quantitative PCR. The reaction mixture (25 μL) contained 0.5 μM each of FTQ-JAK2 and R-JAK2, 1×

TaqMan® Universal PCR Master Mix (Applied Biosystems, CA, USA), 0.2 μM TQ-JAK2, and 1 μL of template DNA. Serial 10-fold dilutions of the PCR product from HEL cells at 10–10^6 copies/μl were used as standard references. The thermal cycling profiles were as follows: 50ºC for 2 min; initial denaturation at 95ºC for 10 min; 50 cycles of denaturation at 95ºC for 40 s, annealing at 58ºC for 40 s, and extension at 72ºC for 40 s. The extracted DNAs were mixed in different proportions (100%, 90%, 80%, 75%, 50%, 30%, 10%, 5%, 1%, and 0% JAK2 allele burdens), which were based on the quantified JAK2 copy numbers.

3.2.5. MPNs patients' DNA

DNAs from 14 MPNs patients attending Juntendo Medical Hospital (Hongo, Tokyo, Japan) and 10 healthy volunteers were used. Institutional Ethics Committee approval was obtained at the institution and written informed consent was obtained from each patient and healthy volunteer. Granulocytes were separated from the blood samples from the patients and healthy volunteers using a RosetteSep® Human Granulocyte Enrichment kit (Stemcell Technologies Inc., Vancouver, Canada) in accordance with the manufacturer's instruction. DNA was extracted from the granulocytes using a QIAamp DNA Mini kit (Qiagen, Hilden, Germany) in accordance with the manufacturer's instruction. After measuring the concentrations of the DNAs using a NanoDrop 1000 spectrophotometer (Thermo Scientific, DE, USA), the DNAs were stored at −80ºC until use.

3.2.6. ABC-PCR

ABC-PCR was performed using a CFX96™ Real-Time PCR detection system (BioRad, CA, USA). The PCR mixture (10 μL) contained 1× titatium Taq DNA polymerase (Clontech, Shiga, Japan), 1.0 μL of 10× titanium buffer, 200 μM each of dNTPs (TaKaRa Bio, Shiga, Japan), 0.12 μM ABP-JAK2, 0.5 μM F-JAK2, 0.15 μM R-JAK2, and 1 μL of template DNA. The PCR conditions were as follows: initial denaturation at 94ºC for 3 min; 50 cycles of denaturation at 94ºC for 30 s, annealing at 62ºC for 30 s, and extension at 72ºC for 30 s; and a final extension at 72ºC for 2 min. PCR was performed in triplicate for each template DNA, and the no-template control (NTC) contained sterilized water instead of the template DNA. After the PCR amplification, the fluorescence intensity of each aliquot was measured at 95ºC and 55ºC. Excitation was performed at 450–490 and 515–535 nm, using 515–530 and 560–580 nm emission filters for green fluorescence and red fluorescence, respectively. Fluorescence raw data were analyzed according to previous studies with slight modification [14, 15]. The fluorescence intensities of the green dye (G_{95}) and red dye (R_{95}) at 95ºC represented the intensities before hybridization, whereas those of the green dye (G_{55}) and red dye (R_{55}) at 55ºC represented the intensities after hybridization. To normalize for non-PCR-related fluorescence intensity fluctuations occurring between reaction tubes, G_{55} and R_{55} were then divided by G_{95} and R_{95}, respectively. The measured fluorescence intensities of the green dye (G_{55}/G_{95}) and red dye (R_{55}/R_{95}) are the sum of the fluorescence intensities from the unbound probe (G_U or R_U), the hybridized probe with the JAK2 wild-type allele (G_{WT} or R_{WT}), and the hybridized probe with the homozygous JAK2V617F allele (G_{V617F} or R_{V617F}). Therefore, G_{55}/G_{95} and R_{55}/R_{95} are expressed respectively as

$[G_{55}/G_{95}] = G_U (1 - y) + G_{WT} [W/(W + M)] y + G_{V617F} [M/(W + M)] y$ (1)

$[R_{55}/R_{95}] = R_U (1 - y) + R_{WT} [W/(W + M)] y + R_{V617F} [M/(W + M)] y.$ (2)

W and M represent the starting quantities of the sequences of the JAK2 wild type and JAK2 mutant type in the individual target, respectively. *y* is the ratio of the amount of the bound probe to the total amount of the probe. In equations (1) and (2), [M/(W + M)] indicates the JAK2 allele burden; therefore, these two equations can be converted to

$[G_{55}/G_{95}] = G_U (1 - y) + G_{WT} [1 - X] y + G_{V617F} X y,$ (3)

and

$[R_{55}/R_{95}] = R_U (1 - y) + R_{WT} [1 - X] y + R_{V617F} X y,$ (4)

where X is the target JAK2 allele burden. At this point,

$R_{WT} = R_{V617F}.$ (5)

Therefore, equation (4) can be converted to

$y = [R_U - (R_{55}/R_{95})]/(R_U - R_{WT}).$ (6)

Substituting the *y* value into equation (3), the following is obtained.

$[(G_{55}/G_{95}) - G_U]/[R_U - (R_{55}/R_{95})] = [(G_{V617F} - G_{WT})/(R_U - R_{WT})] X - [(G_U - G_{WT})/(R_U - R_{WT})]$ (7)

This equation shows that $[(G_{55}/G_{95}) - G_U]/[R_U - (R_{55}/R_{95})]$ and X have a linear relationship.

3.2.7. TaqMan AS-qPCR

TaqMan AS-qPCR was performed using a CFX96™ Real-Time PCR detection system (BioRad, CA, USA). The reaction mixture (15 μL) contained 0.5 μM each of FTQ-JAK2 and R-JAK2 (for the entire JAK2 gene), or 0.5 μM each of FAS-JAK2mt and R-JAK2 (for JAK2V617F gene), 1× TaqMan® Universal PCR Master Mix (Applied Biosystems, CA, USA), 0.2 μM TQ-JAK2, and 1 μL of template DNA. The thermal

cycling profile were as follows: 50ºC for 2 min; initial denaturation at 95ºC for 10 min; 50 cycles of denaturation at 95ºC for 40 s, annealing at 58ºC for 40 s, and extension at 72ºC for 40 s. TaqMan AS-qPCR was performed in triplicate for each template DNA. Results were analyzed using CFX Manager software (BioRad).

3.3. Results

3.3.1. Standard curve for the ABC-PCR

I constructed a standard curve for the quantification of JAK2 allele burden. On the basis of the PCR products from the two cell lines, eight standard mixtures with 1–99% JAK2 allele burdens were prepared at a concentration of 10^5 copies/μl and were used as template DNAs for the analytical validation of ABC-PCR. The template DNA was amplified by PCR, and then the florescence intensity of each aliquot was measured. After measuring the fluorescence intensity, $[(G_{55}/G_{95}) - G_u]/[R_u - (R_{55}/R_{95})]$ was plotted against the JAK2 allele burden of the standard DNA template. The results showed a linear relationship between $[(G_{55}/G_{95}) - G_u]/[R_u - (R_{55}/R_{95})]$ and JAK2 allele burden with a correlation coefficient of $R^2 > 0.996$ for JAK2 allele burdens ranging from 1% to 99% (Figure 3.3).

3.3.2. Flexibility in terms of the initial amount of the template DNA

The ABC-PCR enables the quantification of target JAK2 allele burden regardless of the initial amount of template DNA added into the solution because ABC-PCR is a method based on competitive PCR. The cell line DNAs whose expected JAK2 allele burdens were 30%, 60%, and 75% were subjected to serial 10-fold dilutions to obtain 3.5 ng, 0.35 ng, and 35 pg of cell line DNAs. The JAK2 allele burdens of the serial 10-fold dilutions of the three samples were quantified by ABC-PCR. As a result, the JAK2 allele burdens of the three samples showed excellent agreement with the expected values regardless of the initial amount of the template DNA (Figure 3.4).

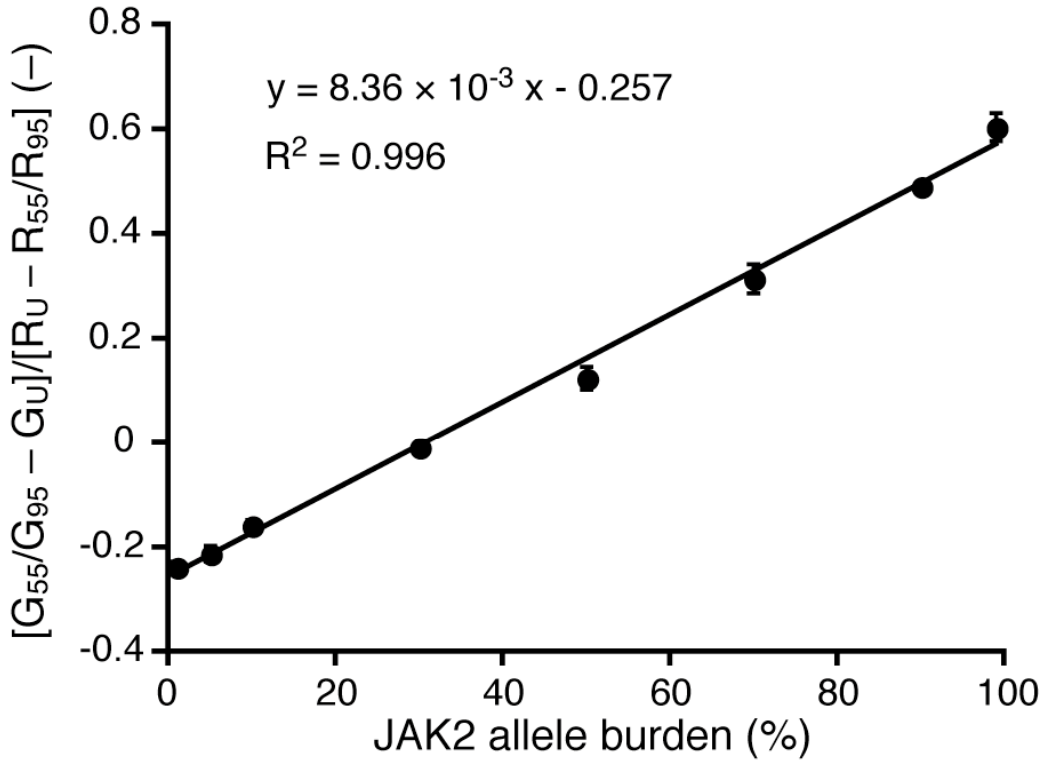

Figure 3.3. Typical standard curve of ABC-PCR for quantifying JAK2 allele burden. A series of samples (99%, 90%, 70%, 50%, 30%, 10%, 5%, and 1% JAK2 allele burden) were amplified in triplicate. G_U and R_U were measured from the fluorescence intensities of the green and red dyes of NTC, respectively. The standard curve was obtained by fitting the data points to a linear relationship. $y = 8.36 \times 10^{-3} x - 0.257$; the correlation coefficient (R^2) was calculated to be 0.996. The error bars represent the standard deviation (SD) of triplicate determinations per dilution.

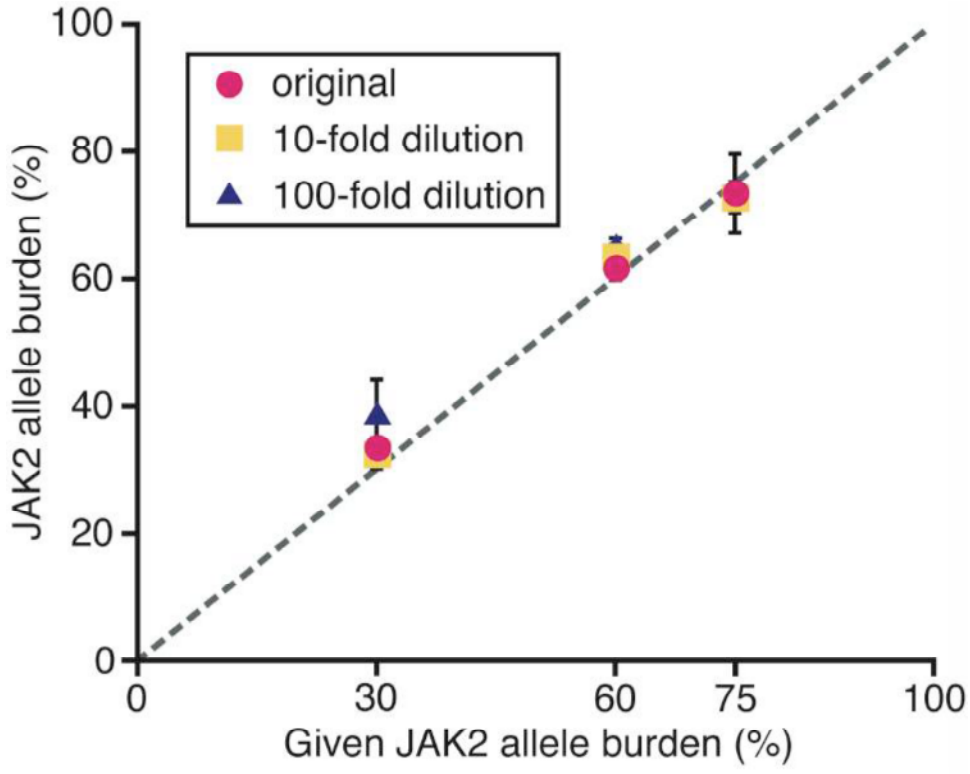

Figure 3.4. The measured JAK2 allele burdens are approximately the same regardless of the initial copy number of the target. The known JAK2 allele burdens of three samples (30%, 60%, and 75%) were quantified by ABC-PCR at different initial amounts (circle, 3.5 ng; square, 0.35 ng; and triangle, 35 pg). Error bars represent the standard deviation of the three replicates. The dashed line corresponds to the expected JAK2 allele burdens.

3.3.3. Comparison with the TaqMan AS-qPCR

The JAK2 allele burdens of the cell line samples were quantified by ABC-PCR and TaqMan AS-qPCR. The cell line samples were a mixture of DNAs from UT-7 and HEL cells with JAK2 allele burdens of 0–100%. The experiments were repeated three times, and mean JAK2 allele burden was calculated. As a result, the JAK2 allele burdens measured by ABC-PCR and TaqMan AS-qPCR were not significantly different (Table 3.2). Moreover, the JAK2 allele burdens measured by ABC-PCR were closer to the expected JAK2 allele burdens in the range of 10–100% than those measured by TaqMan AS-qPCR (Table 3.2). The relative standard deviations (RSDs) of ABC-PCR and TaqMan AS-qPCR were also calculated. The RSDs of ABC-PCR were significantly smaller than those of TaqMan AS-qPCR for the expected JAK2 allele burdens higher than 5% (Table 3.2). However, the RSD of ABC-PCR increased with decreasing measured JAK2 allele burden. The RSDs of TaqMan AS-qPCR varied from 10% to 40% regardless of the corresponding measured JAK2 allele burden (Table 3.2).

Table 3.2. Comparison of the JAK2 allele burdens measured by ABC-PCR and TaqMan AS-qPCR with the expected values

*Expected allele burden (%)	ABC-PCR		TaqMan AS-qPCR	
	Mean ± **SD (%)	†RSD (%)	Mean ± **SD (%)	†RSD (%)
100	99.5 ± 0.3	0.3	> 100	–
90	91.4 ± 0.6	0.6	> 100	–
80	82.6 ± 1.5	1.8	81.3 ± 16.0	19.7
75	78.6 ± 2.1	2.7	82.0 ± 11.3	13.8
50	53.8 ± 2.8	5.3	62.0 ± 8.7	14.1
30	31.2 ± 4.4	3.4	30.5 ± 11.3	37.2
10	11.9 ± 1.2	15	12.3 ± 0.9	7.3
5	7.9 ± 1.1	12.1	6.7 ± 1.3	19.3
1	2.6 ± 1.0	26.3	1.6 ± 0.3	16.4
0	††ND	–	0.8 ± 0.3	42.7

Abbreviations indicated by *, **, †, and †† are as follows: SD, standard deviation; RSD, relative standard deviation; and ND, not determined, respectively.

* Expected JAK2 allele burdens were determined as follows: JAK2 copy numbers of UT-7- and HEL-derived DNAs were quantified by qPCR, and then the DNAs were mixed at intended JAK2 allele burdens.

** Each sample was quantified in triplicate, and its SD was calculated.

† RSD indicates the quantitative assay-to-assay variation. Quantitative experiments by ABC-PCR and TaqMan AS-qPCR were repeated three times, and the RSD of each assay was calculated.

†† The fluorescence intensity was out of range.

3.3.4. The MPNs patients' JAK2 allele burden

The JAK2 allele burdens in the 14 MPNs patients and 10 healthy volunteers were quantified by ABC-PCR. The experiments were repeated three times, and the measured JAK2 allele burdens were calculated. TaqMan AS-qPCR was also applied to the same samples, and the values obtained by the two assays were compared. As a result, the JAK2 allele burdens measured by ABC-PCR and TaqMan AS-qPCR were approximately the same (Figure 3.5). In the case of the MPNs cohort, most of the RSDs of ABC-PCR were smaller than those of TaqMan AS-qPCR (Figure 3.5 and Table 3.3). In contrast, the JAK2 allele burdens of the healthy cohort measured by ABC-PCR were larger than those measured by TaqMan AS-qPCR (0–7% determined by ABC-PCR, 0.8% at most determined by TaqMan AS-qPCR) (Table 3.3).

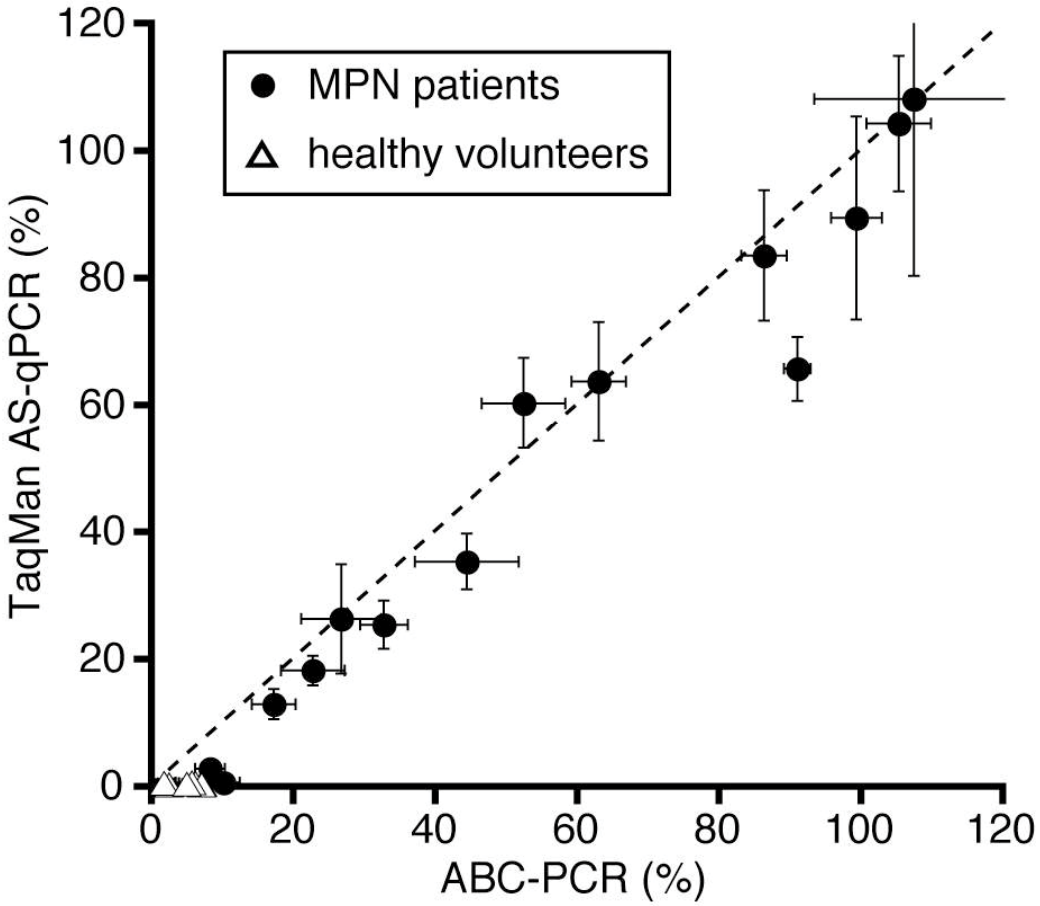

Figure 3.5. JAK2 allele burden in the 14 patients with MPNs and 10 healthy volunteers in this study. Solid circles represent the JAK2 allele burdens of individual patients with MPNs. Open triangles represent the JAK2 allele burdens of healthy volunteers. The horizontal axis represents the values measured by ABC-PCR, and the vertical axis represents those measured by TaqMan AS-qPCR. The dashed line represents the same measured values between the two methods. The horizontal and vertical error bars represent the standard deviations of ABC-PCR and TaqMan AS-qPCR, respectively.

Table 3.3. JAK2 allele burdens of 14 MPNs cohort and 10 healthy cohort

sample No.	ABC-PCR		TaqMAn AS-qPCR	
	MEAN ± *SD (%)	**RSD (%)	MEAN ± *SD (%)	**RSD (%)
1	99.2 ± 3.6	3.6	89.6 ± 15.9	17.8
2	>100	13.1	>100	25.7
3	86.2 ± 3.2	3.7	83.7 ± 10.2	12.2
4	90.9 ± 1.9	2.1	65.9 ± 5.0	7.6
5	52.3 ± 5.9	11.2	60.5 ± 7.1	11.7
6	>100	4.4	>100	10.2
7	22.6 ± 4.5	19.9	18.4 ± 2.3	12.6
8	17.1 ± 3.1	18.1	13.1 ± 2.4	17.9
9	44.3 ± 7.3	16.5	35.5 ± 4.4	12.3
10	26.6 ± 5.6	21.2	26.5 ± 8.6	32.4
11	8.1 ± 2.1	25.5	3.0 ± 0.8	25.2
12	62.9 ± 3.8	6.1	63.9 ± 9.4	14.6
13	10.0 ± 2.3	23.1	0.8 ± 0.1	16.1
14	32.6 ± 3.3	10.2	25.6 ± 3.8	14.7
15	0.2 ± 2.5	1250	1.0 ± 0.3	32.7
16	6.9 ± 3.2	46.4	0.7 ± 0.2	30
17	6.0 ± 2.2	37	0.7 ± 0.2	27.1
18	6.0 ± 4.4	73.9	0.7 ± 0.2	23.7
19	7.0 ± 2.8	40.7	0.6 ± 0.1	21
20	6.9 ± 2.3	33.6	0.5 ± 0.2	46.1
21	5.5 ± 2.2	40.4	0.8 ± 0.2	27.1
22	2.3 ± 3.6	152	0.5 ± 0.3	52.5
23	1.6 ± 1.5	91.3	0.7 ± 0.3	35.4
24	4.8 ± 2.0	42	0.6 ± 0.4	66.2

Sample numbers 1 to 14 indicate MPNs cohort (colored in white), sample numbers 15 and higher indicate healthy cohort (colored in gray).

Abbreviations indicated by * and ** are as follows: SD, standard deviation and RSD, relative standard deviation, respectively.

* Each sample was quantified in triplicate, and its SD was calculated.

** RSD indicates the quantitative assay-to-assay variation. Quantitative experiments by ABC-PCR and TaqMan AS-qPCR were repeated three times, and the RSD of each assay was calculated.

3.4. Discussion

The development of a simple, cost-effective, and accurate method for quantifying JAK2 allele burden is expected to contribute to the monitoring of JAK2V617F-positive MPNs following stem cell transplantation or administration of soon-to-be-available JAK2 inhibitors. In this study, we propose ABC-PCR as such a method. We first constructed the ABC-PCR standard curve, then we validated the range of target JAK2 allele burdens that can be accurately quantified by ABC-PCR using DNAs extracted from cell lines. In addition, we quantified the JAK2 allele burdens in patients with MPNs by ABC-PCR and TaqMan AS-qPCR. Finally, we discuss the characteristics of ABC-PCR in terms of operative complexity, running cost, and accuracy of quantification.

The standard curves for ABC-PCR showed a linear relationship between $[(G_{55}/G_{95}) - G_U]/[R_U - (R_{55}/R_{95})]$ and JAK2 allele burden (Figure 3.3). The standard curve had a correlation coefficient (R^2) of at least 0.996 and an SD of less than 0.049. The results indicate that ABC-PCR can be used for quantification and can reproducibly measure JAK2 allele burden. Furthermore, ABC-PCR can be performed using a common thermal cycler and a simple fluorometer, and target JAK2 allele burden can be quantified regardless of the initial amount of the target DNA added into the solution (Figure 3.4). Moreover, target JAK2 allele burden can be quantified in a single reaction because the G allele (JAK2 wild type) causes a dose-dependent decrease in the fluorescence intensity of the AB-Probe. Taken together, the throughput of ABC-PCR is approximately twice as high as that of TaqMan AS-qPCR; moreover, the running cost can be reduced to half.

The RSDs were no more than 15% for JAK2 allele burdens ≥5% in the DNAs extracted from the cell lines (Table 3.2). However, the RSD at 1% JAK2 allele burden was markedly high, i.e., 26.3% (Table 3.2). At low JAK2 allele burdens, almost all of the JAK2 alleles are G alleles; therefore, the green fluorescence intensity notably decreases. In this situation, the small fluctuation of fluorescence intensity causes large quantitative errors. Therefore, ABC-PCR may lack accuracy of quantification of JAK2 allele burdens less than 5%. On the other hand, ABC-PCR is more accurate than TaqMan AS-qPCR for JAK2 allele burdens ≥10%. The JAK2 allele burdens measured by ABC-PCR were quite close to the expected values ≥10% (Table 3.2). In contrast, those measured by TaqMan AS-qPCR varied widely in this range (Table 3.2). In TaqMan AS-qPCR, JAK2 allele burden is calculated by dividing the copy number of the JAK2V617F allele by that of the total JAK2 alleles. The copy number of each allele is quantified by separate assays; therefore, amplification efficiency may differ in each reaction. The fluctuation of amplification efficiency may cause the quantitative variation in TaqMan AS-qPCR. In particular, we were unable to differentiate between the known JAK2 allele burdens of 75% and 80% by TaqMan AS-qPCR, whereas we were able to fairly differentiate them in ABC-PCR (Table 3.2). These findings suggest that ABC-PCR is more accurate than TaqMan AS-qPCR when the target JAK2 allele burdens are ≥10%, although the lower quantification limit of ABC-PCR is not as much as that of TaqMan AS-qPCR. It would be crucial that a target JAK2 allele burden ≥10%, particularly around 50%, can be accurately quantified with a small assay-to-assay quantitative variation because patients whose JAK2 allele burden is >50% are at a much higher risk of their PV progressing to PMF than patients whose JAK2 allele burden is <50% [18].

In the case of the healthy cohort, the JAK2 allele burdens measured by ABC-PCR were generally higher than those measured by TaqMan AS-qPCR (Table 3.3). The reason for this result is similar to that for the experiments performed using the cell line DNAs. That is, a small fluorescent fluctuation causes large errors. A cross check using other methods would be required when the JAK2 allele burden measured by ABC-PCR is around 10%. This check is required not only for ABC-PCR but also for TaqMan AS-qPCR. For example, the JAK2 allele burdens of the sample Nos. 13 and 15 measured by TaqMan AS-qPCR were 0.8% and 1.0%, respectively; however, sample No. 13 was from an MPN patient and sample No. 15 was from a healthy volunteer (Table 3.3). The diagnosis of the patients with low JAK2 allele burdens should be considered carefully. In the clinical study of the MPNs cohort, no significant difference was observed between the JAK2 allele burdens measured by ABC-PCR and those measured by TaqMan AS-qPCR when the JAK2 allele burdens were >10% (Figure 3.5). Furthermore, most of the RSDs of ABC-PCR were smaller than those of TaqMan AS-qPCR (Table 3.3). These findings suggest that the adequacy of ABC-PCR for quantification is proved not only retrospectively but also prospectively. This means that ABC-PCR has potential use for quantifying the JAK2 allele burdens of unknown samples fairly accurately.

3.5. Conclusion

In summary, we have established a simple, cost-effective, and accurate JAK2 allele burden quantification method by ABC-PCR. The method can be performed using a simple thermal cycler and a fluorometer without optimizing the initial amount of target DNA; moreover, the method can accurately quantify the target JAK2 allele burdens ≥10%. ABC-PCR has a potential to be used as a powerful tool for quantifying JAK2

allele burden.

References

1. Baxter EJ, Scott LM, Cambell PJ, East C, Fourouclas N, Swanton S, et al. Acquired mutation of the tyrosine kinase JAK2 in human myeloproliferative disorders. *Lancet* 2005; **365:** 1054-61
2. James C, Ugo V, Le Couédic JP, Staerk J, Delhommeau F, Lacout C, et al. A unique clonal JAK2 mutation to constitutive signaling causes polycythemia vera. *Nature* 2005; **434:** 1144-8.
3. Levine RL, Wadleigh M, Cools J, Ebert BL, Wernig G, Huntly BJP, et al. Activating mutation in the tyrosine kinase JAK2 in polycythemia vera, essential thrombocythemia, and myeloid metaplasia with myelofibrosis. *Cancer Cell* 2005; **7:** 387-97.
4. Campbell PJ and Green AR. The myeloproliferative disorders. *New Engl. J. Med.* 2006; **355:** 2452-66.
5. Schnittger S, Backer U, Haferlach C, Geer T, Müller P, Mittermüller J, et al. Detection of JAK2 exon 12 mutations in 15 patients with JAK2V617F negative polycythemia vera. *Haematologica* 2009; **94:** 414-8.
6. Tefferi A, and Vardiman JW. Classification and diagnosis of myeloproliferative neoplasms: the 2008 World Health Organization criteria and point-of-case diagnostic algorithms. *Leukemia* 2008; **22:** 14-22.
7. Passamonti F, and Rumi E. Clinical relevance of JAK2 (V617F) mutant allele burden. *Haematologica* 2009; **94:** 7-10.
8. Tiedt R, Hao-Shen H, Sobas MA, Looser R, Dirnhofer S, Schwaller J, et al. Ratio of mutant JAK2-V617F to wild-type JAK2 determines the MPD phenotypes in transgenic mice. *Blood* 2008; **111:** 3931-40.
9. Cardama QA, Vaddi K, Liu P, Manshouri T, Li J, Scherle PA, et al. Preclinical

characterization of the selective JAK1/2 inhibitor INCB018424: therapeutic implications for the treatment of myeloproliferative neoplasms. *Blood* 2010; **115:** 3109-17.

10. Wernig G, Kharas MG, Okabe R, Moore SA, Leeman DS, Cullen DE, et al. Efficiency of TG101348, a selective JAK2 inhibitor, in treatment of a murine model of JAK2V617F-induced polycythemia vera. *Cancer Cell* 2008; **13:** 311-20.
11. Tanaka R, Kuroda J, Stevenson W, Ashihara E, Ishikawa T, Taki T, et al. Fully automated and super-rapid system for the detection of JAK2V617F mutation. *Leuk. Res.* 2008; **32:** 1462-7.
12. Larsen TS, Christensen JH, Hasselbalch HC, and Pallisgaard N. The JAK2 V617F mutation involves B- and T-lymphocyte lineages in a subgroup of patients with Philadelphia-chromosome negative chronic myeloproliferative disorders. *Br. J. Haematol.* 2007; **136:** 745-51.
13. Lippert E, Girodon F, Hammond E, Jelinek J, Reading NS, Fehse B, et al. Concordance of assays designed for the quantification of JAK2V617F: a multicenter study. *Haematologica* 2009; **94:** 38-45.
14. Tani H, Kanagawa K, Kurata S, Teramura T, Nakamura K, Tsuneda S, et al. Quantitative method for specific nucleic acid sequences using competitive polymerase chain reaction with an alternately binding probe. *Anal. Chem.* 2007; **79:** 974-9.
15. Miyata R, Adachi K, Tani H, Kurata S, Nakamura K, Tsuneda S, et al. Quantitative detection of chloroethene-reductive bacteria *Dehalococcoides* spp. using alternately binding probe competitive polymerase chain reaction. *Mol. Cell. Probes* 2010; **24:** 131-7.
16. Torimura M, Kurata S, Yamada K, Yokomaku T, Kamagata Y, Kanagawa T, et al.

Fluorescence-quenching phenomenon by photoinduced electron transfer between a fluorescent dye and a nucletide base. *Anal. Sci.* 2001; **17:** 155-60.

17. Rapado I, Albizua E, Ayala R, Herinández JA, Garcia-Alonso L, Grande S, et al. Validity test of JAK2 V617F and allele burden quantification in the diagnosis of myeloproliferative disorders. *Ann. Hematol.* 2008; **87:** 741-9.
18. Passamonti F, Rumi E, Pietra D, Elena C, Boveri E, Arcaini L, et al. A prospective study of 338 patients with polycythemia vera: the impact of JAK2 (V617F) allele burden and leukocytosis on fibrotic or leukemic disease transformation and vascular complications. *Leukemia* 2010; **24:** 1574-9.

Chapter 4

Digital PCR is appropriate as the primary measurement of the standard samples for nucleic acid quantification

Chapter 4

Digital PCR is appropriate as the primary measurement of the standard samples for nucleic acid quantification

4

4.1. Introduction

Almost all of the methods including quantitative polymerase chain reaction (qPCR) [1-3] and alternately binding probe competitive PCR (ABC-PCR) [4] require standard samples for the quantification of nucleic acids of the interests. Such methods are always shadowed by the uncertainty derived from the variations of standard samples. Several absolute quantification methods such as an absorbance measurement do not require standard samples; however, these methods cannot quantify the amount of particular target. Recently, an innovative method named digital PCR, that achieves the absolute quantification of the nucleic acids of the interest has been developed [5, 6]. Target absolute copy number can be quantified using digital PCR by directly counting the positive signals of partitions; therefore, no standard samples are required. Furthermore, the method can determine the difference of few copy numbers of the target. Because of its quantitative accuracy and sensitivity, the digital PCR is also used for the clinical applications or the investigation of the number of library molecules applied to next-generation sequencing [7-9]. However, the method has limitations at the point of throughput and running cost. Further technological developments are ongoing to

overcome these shortcomings [10, 11]; however, it is still difficult to use the method in practical.

Here, I have constructed the standard samples for ABC-PCR using digital PCR. ABC-PCR can be used as a simple, cost-effective, and accurate JAK2 allele burden quantification. However, ABC-PCR requires standard samples of which JAK2 allele burdens are rigidly defined because the variations from the standard samples critically causes the large deviations from the expected values. Utilizing digital PCR, JAK2 allele burdens of the standard samples for ABC-PCR are strictly determined. Therefore, such usage of the digital PCR would contribute to not only the increase of the quantitative reliability of ABC-PCR but also the restraint on the digital PCR.

In this study, I have constructed the rigidly validated standard samples for ABC-PCR to quantify the JAK2 allele burden. First, the extracted DNAs from UT-7 and HEL cell lines were amplified using PCR and the concentrations of the amplified products were determined using digital PCR. Then the PCR products were mixed with different proportions based on the JAK2 copy numbers. Finally ABC-PCR was performed to the cell line DNAs with given JAK2 allele burdens using the standard samples calibrated by digital PCR and other two methods, and then the measured values of each method were compared.

4.2. Materials and Methods

4.2.1. Cell lines

UT-7 cell lines, which have homozygous JAK2 wild type alleles, and HEL cell lines, which have homozygous JAK2V617F alleles, were used in this study. UT-7 was cultured in IMDM medium (GIBCO, MD, USA) with 10% fetal calf serum (FCS) (GIBCO), 10 ng/ml erythropoietin (EPO), 100 units/ml of penicillin (GIBCO), and 100 μg/ml of streptomycin (GIBCO) at 37ºC in 5% CO_2. HEL was cultured in RPMI 1640 medium (SIGMA, MO, USA) with 10% FCS (GIBCO), 10 ng/ml EPO, 100 units/ml of penicillin (GIBCO), and 100 μg/ml of streptomycin (GIBCO) at 37ºC in 5% CO_2. EPO was kindly provided by Kyowa Hakko Kirin, Tokyo, Japan. Medium change was conducted every 3 days.

4.2.2. Oligonucleotides

The sequences of primers, probes are listed in Table 4.1. All the primers were purchased from Tsukuba Oligo Services Co., Ltd., Ibaraki, Japan. The AB-Probe labeled at a 5′ end with TAMRA and at a 3′ end with BODIPY FL was purchased from J-Bio 21 Corp., Ibaraki, Japan. The TaqMan probe was purchased from Applied Biosystems, CA, USA. The specificity of the primers, AB-Probe, and TaqMan probe were verified by a database search using BLAST from the DNA data bank of Japan (DDBJ).

Table 4.1. Oligonucleotide primers and probes used in this study

Name	Sequence (5'–3')	*Position	Used for	Note	Reference
Primer					
F-JAK2-std	cac ttt gat ctc cat att cca g	54772–54793	Standard sample construction	Forward primer for both JAK2 alleles	**this study
R-JAK2-std	ctg cca taa tct ctt ttg c	55365–55347	Standard sample construction	Reverse primer for both JAK2 alleles	**this study
F-JAK2	atc tat agt cat gct gaa agt agg aga aag	54871–54900	ABC-PCR	Forward primer for both JAK2 alleles	10
FTQ-JAK2	tga tga gca agc ttt ctc ac	55011–55030	TaqMan AS-qPCR	Forward primer for both JAK2 alleles	**this study
FAS-JAK2wt	agc att tgg ttt taa att atg gag tat atc	55032–55061	TaqMan AS-qPCR	Forward primer for JAK2 wild type allele	**this study
FAS-JAK2mt	agc att tgg ttt taa att atg gag tat att	55032–55061	TaqMan AS-qPCR	Forward primer for JAK2 mutant allele	10
R-JAK2	ctg aat agt cct aca gtg ttt tca gtt tca	55234–55205	ABC-PCR/TaqMan AS-qPCR	Reverse primer for both JAK2 alleles	10
Probe					
ABP-JAK2	(TAMRA)-cct gta gtt tta ctt act ctc gtc tcc aca ga-(BODIPY)	55093–55062	ABC-PCR	AB-Probe	**this study
TQ-JAK2	(FAM)-tgt gga gac gag agt aa-(MGB)	55064–55080	TaqMan AS-qPCR	TaqMan Probe	11

* The position is based on the sequence obtained from GenBank Accession No. AL161450.
** The specificities of all the primers and probes designed in this study were validated by a database search using BLAST from the DNA data bank of Japan (DDBJ).

4.2.3. DNA extraction

Each of the UT-7 and the HEL culture was centrifuged at 200 × g for 5 min, and then the supernatant was removed. The cell lines were resuspended in 2 mL of phosphate buffered saline (PBS) (GIBCO) and then DNAs were extracted from UT-7 and HEL cell lines using a QIAamp DNA Mini kit (Qiagen, Hilden, Germany) according to the manufacturer's instructions. The concentrations of the extracted DNAs were measured using a NanoDrop 1000 spectrophotometer (Thermo Scientific, DE, USA). The extracted DNAs were then amplified by PCR using Veriti® 96-well Thermal Cycler (Applied Biosystems, CA, USA) to obtain a 597 bp DNA fragment. The reaction mixture (50 μL) contained 1× TaKaRa Taq HS (TaKaRa Bio, Shiga, Japan), 5.0 μL of 10× PCR buffer, 200 μM each of dNTPs mix (TaKaRa Bio), 0.5 μM each of F-JAK2-std and R-JAK2-std, and 1 μL of extracted DNA. The PCR conditions were as follows: initial denaturation at 95ºC for 2 min; 30 cycles of denaturation at 95ºC for 30 s, annealing at 58ºC for 30 s, and extension at 72ºC for 40 s; and a final extension at 72ºC for 2 min. Subsequently, the PCR products were purified using a Microcon YM-50 (Millipore, MA, USA). The fragment length and approximate concentration of the purified products were estimated using a NanoDrop 2000 spectrophotometer (Thermo Scientific) and an Agilent 2100 Bioanalyzer (Agilent Technologies, CA, USA).

4.2.4. Digital PCR

Digital PCR was performed using the 12.765 Digital Arrays on the BioMark System (Fluidgm, CA, USA). The array provides 4.6 μL of reaction mixture into 765 individual partitions (approximately 6.0 nL per partition) using the NanoFlex IFC Controller (Fluidigm). The PCR reaction mix (10 μL) contains 1 × TaqMan Universal Master Mix II (Applied Biosystems), 1 × GE sample loading reagent (Fluidigm), 0.5 μM of each

FTQ-JAK2 and R-JAK2, 200 nM of TQ-JAK2, and 1 μL template DNA. The DNA samples were gravimetrically diluted to 300 copies based on the values by the Agilent 2100 Bioanalyzer (Agilent Technologies). After dispensing the reaction mixture to the partitions, the massively parallel PCR was performed. The PCR thermal conditions is as follows: 50ºC for 2 min, 95ºC for 10 min, 45 cycles of 40 sec at 95ºC for denaturation, 40 sec at 58ºC for annealing, and 40 sec at 72ºC for extension. After the PCR amplification, the digital the fluorescence intensity of each partition was measured using the BioMark System EP1 (Fluidigm). The data was analyzed using Digital PCR analysis software ver. 2.1 (Fluidigm).

4.2.5. Standard samples

The PCR products obtained from UT-7 and HEL cell lines were mixed in different proportions (99%, 90%, 70%, 50%, 30%, 10%, 5% and 1% of JAK2 allele burdens), of which concentrations were 10^5 copies/μl. The standard samples were prepared based on the copy number derived from the NanoDrop 2000 spectrophotometer (Thermo Scientific), the Agilent 2100 Bioanalyzer (Agilent Technologies), and the digital PCR (Fluidigm).

4.2.6. ABC-PCR

The PCR mixture (25 μL) contained 1× titanium Taq DNA polymerase (Clontech, Shiga, Japan), 2.5 μL of 10× titanium buffer, 200 μM each of dNTPs mix (TaKaRa Bio), 0.12 μM of ABP-JAK2, 0.5 μM of F-JAK2, 0.15 μM of R-JAK2, and 1 μL of template DNA. PCR amplification was performed using Veriti® 96-well Thermal Cycler (Applied Biosystems) with the following program: initial denaturation at 94ºC for 3 min; 50 cycles of denaturation at 94ºC for 30 s, annealing at 62ºC for 30 s, and

extension at 72ºC for 30 s; and a final extension at 72ºC for 2 min. The PCR was performed in triplicate for each template DNA, and the no-template control (NTC) contained sterilized water instead of the template DNA. After the PCR amplification, the fluorescence intensity of each aliquot was measured by use of LightCycler480 (Roche Diagnostics, Basel, Switzerland) at 95ºC and 55ºC. Excitation was performed at 450–495 and 522–555 nm, using 505–537 and 565–605 nm emission filters for green fluorescence and red fluorescence, respectively. The fluorescence raw data was analyzed according to the description in Chapter 3.

4.3. Results

4.3.1. DNA concentration

DNAs extracted from UT-7 and HEL cell lines were amplified using PCR, then the concentrations of the PCR products were quantified using the NanoDrop 2000 spectrophotometer (Thermo Scientific) and the Agilent 2100 Bioanalyzer (Agilent Technologies). The DNA concentrations were converted into the copy number using the following equation:

$$C_N = [x \times 10^{-9} \times N_A]/[A \times B]$$

where C_N: copy number [copies/μl], x: DNA concentration [g/μl], N_A: Avogadro's number [copies/mol], A: length of the amplicon [bp], B: average molecular weight of a base pair [Da].

The copy number by the digital PCR (Fluidigm) was quantified as follows. The number of the positive partitions was counted from the plate image (Figure 4.1) and the number was treated with the Poisson distribution to obtain the estimated copy number of the target. Each method was performed in quintuplicate, and the mean and the standard deviations (SDs) were calculated. The estimated copy number of the PCR products by the three samples was slightly different from each other (Table 4.2). The amount derived from HEL was generally greater than that of UT-7.

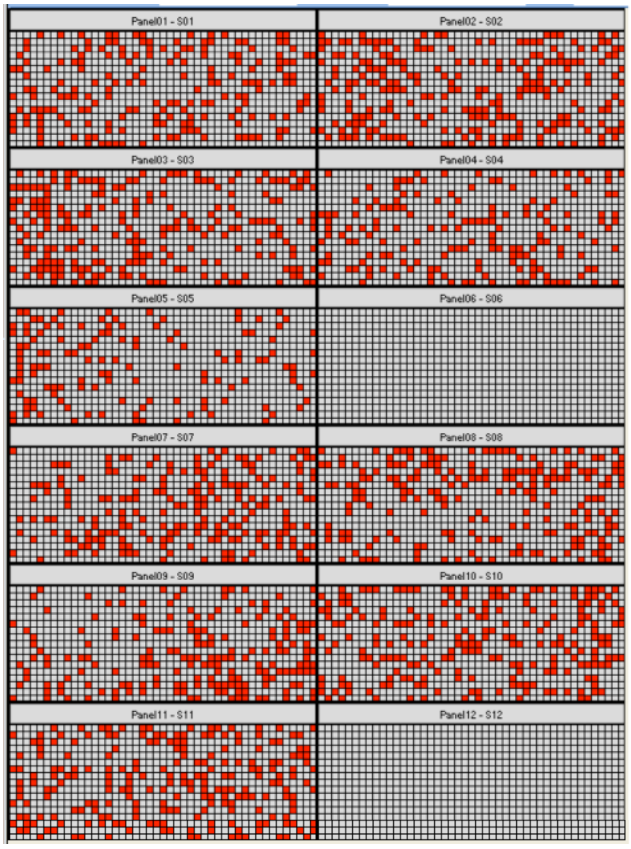

Figure 4.1. Plate image of digital PCR. Each panel is separated to 765 partitions. The reaction mixture (6.0 nL) was dispensed to each partition, and then the massive simultaneous PCR was performed. Red dots represent the hit partitions, which include the JAK2 DNA. Gray dots represent the non-hit partitions. After counting the hit partitions of each panel, estimated copy number of the target was quantified by dealing the counts with Poisson distribution. Panel 01–05; PCR product derived from DNA extracted from UT-7 cell line. Panel 07–11; PCR product derived from DNA extracted from HEL cell line. Panel 06 and 12; no-template control.

Table 4.2. JAK2 copy number by the three methods.

method	copy number (copies)	
	UT-7	HEL
digital PCR	3.9×10^{11}	5.7×10^{11}
Agilent 2100	2.4×10^{11}	3.2×10^{11}
NanoDrop 2000	5.7×10^{11}	6.6×10^{11}

4.3.2. JAK2 allele burdens of the standard samples

Standard samples were constructed by mixing the PCR products derived from UT-7 and HEL, based on the copy numbers by the three methods. The combined use of the TaqMan AS-qPCR and the digital PCR (digital AS-PCR) was performed to validate the JAK2 allele burdens of the standards by digital PCR. Two Allele Specific primers (FAS-JAK2mt for JAK2V617F gene, and FAS-JAK2wt for JAK2 wild type gene) were used as the forward primers instead of the use of FTQ-JAK2 primer in the digital AS-PCR. The digital AS-PCR assay revealed that the standard samples certainly indicated the values around the expected JAK2 allele burdens (Table 4.3).

Table 4.3. JAK2 allele burdens of the standard samples validated by the digital AS-PCR

expected JAK2 allele burden (%)	copy number (copies)		**JAK2 allele burden (%)**
	UT-7	HEL	
100	30	65344	**100.0**
99	528	58046	**99.1**
90	5037	36503	**87.9**
70	11089	20828	**65.3**
50	13886	16524	**54.3**
30	30035	16657	**35.7**
10	48398	4371	**8.3**
5	42682	2414	**5.4**
1	41798	528	**1.2**
0	43064	50	**0.1**

4.3.3. Comparison of the measured JAK2 allele burdens with the three standards

The standard curves for ABC-PCR were constructed. Three series of the standard samples were used. Each standard was prepared based on the copy numbers shown in Table 4.2, ranging from 1–99% JAK2 allele burdens at a concentration of 10^5 copies/μl. The three standard curves were fitted to linear relationships with similar slope/intercept (Figure 4.2).

ABC-PCR was performed by use of the standard samples derived from three methods. The cell line DNAs with given JAK2 allele burden (0%, 1%, 5%, 10%, 20%, 60%, and 95%) were quantified by using the each standard curve. The SDs of the targets were also calculated. The measured JAK2 allele burdens by the three standards indicated approximately the same values although the values from the Agilent 2100 Bioanalyzer were slightly higher than those from other two methods (Table 4.4).

Table 4.4. Measured JAK2 allele burdens by the three standard samples

expected allele burden (%)	digital PCR		Agilent 2100		NanoDrop 2000	
	JAK2 allele burden (%)	SD (%)	JAK2 allele burden (%)	SD (%)	JAK2 allele burden (%)	SD (%)
95	**93.1**	0.74	**95.4**	0.75	**93.6**	0.75
60	**63.0**	0.76	**65.2**	0.76	**63.0**	0.77
20	**24.4**	2.39	**26.4**	2.40	**23.9**	2.42
10	**11.2**	0.30	**13.1**	0.30	**10.5**	0.30
5	**4.7**	0.92	**6.6**	0.93	**3.9**	0.93
1	**N. D.**	0.61	**1.4**	0.61	**N. D.**	0.62
0	**N. D.**	1.61	**0.5**	1.62	**N. D.**	1.63

N. D: not determined. The fluorescence intensity was out of range.

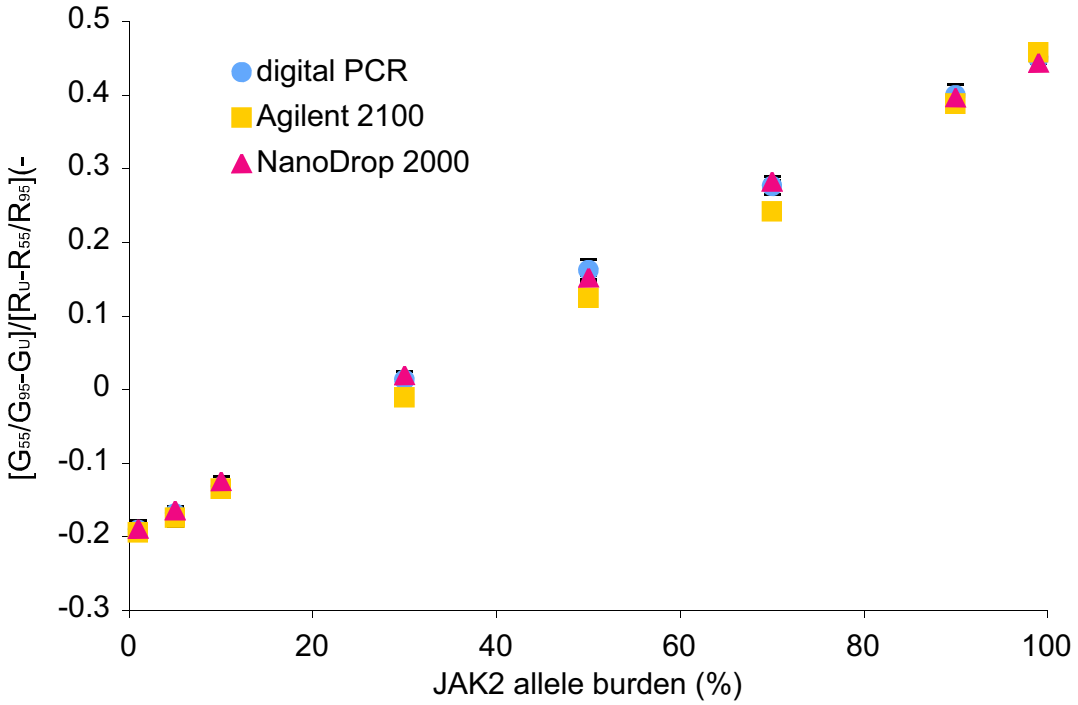

Figure 4.2. Standard plots obtained from the three methods. Azure circle: standard samples validated by use of the digital PCR. The standard curve was fitted to the linear relationship between the JAK2 allele burden and the $[G_{55}/G_{95} - G_U]/[R_U - R_{55}/R_{95}]$ value. $y = 6.6 \times 10^{-3}\ x - 0.193$; the correlation coefficient (R^2) was calculated to be 0.998. Yellow square: standard samples validated by use of the Agilent 2100 Bioanalyzer. The standard curve was obtained as the same to the digital PCR. $y = 6.6 \times 10^{-3}\ x - 0.205$; the correlation coefficient (R^2) was calculated to be 0.999. Fuchsia triangle: standard samples validated by use of the NanoDrop 2000 spectrophotometer. The standard curve was expressed as $y = 6.5 \times 10^{-3}\ x - 0.188$; the correlation coefficient (R^2) was calculated to be 0.998. The error bars represent the standard deviation (SD) of triplicate determinations per dilution.

4.4. Discussion

It is very important to construct the standard samples of which expected values are rigidly determined for improving the reliability and the certainty of the quantitative methods. However, no methods existed that can be utilized to validate the own values of the standard samples. Digital PCR is such the promising method because the method can be performed to quantify target DNA/RNA without using the standard samples. In this study, the standard samples for the quantification of the JAK2 allele burden were constructed using the digital PCR. Three series of standard samples were constructed by mixing two PCR products, based on the copy number that was determined using the digital PCR, the Agilent 2100 Bioanalyzer, and the NanoDrop 200 spectrophotometer. The ABC-PCR was performed to the cell line DNAs with given JAK2 allele burdens by use of the three standard series, and then the measured values of each method were compared.

The each estimated copy number of the PCR products was different depending on the measurement methods although the products were the same samples (Table 4.2). The numbers in decreasing order were the ones by the NanoDrop 2000 spectrophotometer, by the digital PCR, and by the Agilent 2100 Bioanalyzer. The shift is caused from the uncertainty of each measurement method. In the NanoDrop 2000 spectrophotometer, the concentration of the target is quantified using the absorbance. Therefore, the non nucleic acids specific absorbance causes the overestimation of the value. The Agilent 2100 Bioanalyzer is the method based on the requirement of the sample. Such method often causes the measurement shift from the expected value. The digital PCR also has several uncertainties such as the PCR bias. The results suggest that the cross check using the plural methods is essential for improving the reliability of the measured

values.

Contrastingly, the standard curves obtained from the three standard series were fitted to the similar linearity (Figure 4.2). Furthermore, the measured JAK2 allele burdens of the cell line DNAs by the standards showed no significant differences (Table 4.4). I simulated the JAK2 allele burdens of the standard based on the copy numbers determined by the Agilent 2100 and the NanoDrop 2000 spectrophoeter, assuming the numbers by the digital PCR are the true values. The PCR products from UT-7 DNA were diluted 2.4×10^6-fold in the case of the Agilent 2100 Bioanalyzer, and 3.2×10^6-fold in the case of the NanoDrop 2000 spectrophotometer. As a result, the true copy number of the PCR products were 1.6×10^5 copies/μl in the Agilent 2100 Bioanalyzer, and 0.7×10^5 copies/μl in the NanoDrop 2000 spectrophotometer. Likewise, the true copy number of the PCR products from HEL were 1.8×10^5 copies/μl in the Agilent 2100 Bioanalyzer, and 0.8×10^5 copies/μl in the NanoDrop 2000 spectrophotometer. Calculating the true JAK2 allele burdens of the standard samples based on these copy numbers, the true JAK2 allele burden shifted approximately 3% higher than the expected JAK2 allele burden in maximum (Table 4.5 and 4.6). The maximum shift caused at the JAK2 allele burden around 50%. In contrast, the shift was quite small (1% at most) at the high or low JAK2 allele burdens (Table 4.5 and 4.6). The trend by the simulation was good agreement with the result obtained from the experiment (Figure 4.2). This suggests that the measured JAK2 allele burdens may contain a little uncertainty depending on the standard samples in ABC-PCR. The shift is considered quite little; however, it is also suggested that the shift possibly causes serious quantitative variation to the true value in the case of the copy number quantification such as quantitative PCR. From the simulation based on the experimental values, it is

possible that the measured copy number indicates approximately twice as high value as the true value (Table 4.5, HEL copy number column). Therefore, I considered that the cross check by use of the plural methods to the standard samples is crucial to minimize the effect derived from the standard samples.

Table 4.5. Simulated copy numbers and the JAK2 allele burdens by the Agilent 2100 Bioanalyzer

expected JAK2 allele burden (%)	copy number (copies)		true JAK2 allele burden (%)
	UT-7	HEL	
99	1.6×10^3	1.8×10^5	99.1
90	1.6×10^4	1.6×10^5	90.9
70	4.8×10^4	1.3×10^5	73.0
50	8.0×10^4	9.0×10^4	53.0
30	1.1×10^5	5.4×10^4	33.0
10	1.4×10^5	1.8×10^4	11.3
5	1.5×10^5	9.0×10^3	5.7
1	1.6×10^5	1.8×10^3	1.1

Table 4.6. Simulated copy numbers and the JAK2 allele burdens by the NanoDrop 2000 spectrophotometer

expected JAK2 allele burden (%)	copy number (copies)		true JAK2 allele burden (%)
	UT-7	HEL	
99	7.0×10^2	7.9×10^4	99.1
90	7.0×10^3	7.2×10^4	91.1
70	2.1×10^4	5.6×10^4	72.7
50	3.5×10^4	4.0×10^4	53.3
30	4.9×10^4	2.4×10^4	32.9
10	6.3×10^4	8.0×10^3	11.3
5	6.7×10^4	4.0×10^3	5.6
1	6.9×10^4	8.0×10^2	1.1

4.5. Conclusion

In this study, the standard samples were constructed by use of the three methods. It is strongly suggested that the standard samples for the quantification of the nucleic acids should be checked carefully by use of plural methods. The trend will be the global standard because the validation methodology for the standard samples is not established in the field of life science so far.

References

1. Morrison T. B., Weis J. J., and Witter C. T. Quantification of low-copy transcripts by continuous SYBR® green I monitoring during amplification. *Biotechniques* 1998; **24:** 954-62.
2. Lee L. G., Connell C. R., and Bloch W. Allelic discrimination by nick-translation PCR with fluorogenic probes. *Nucleic Acids Res.* 1993; **21:** 3761-6.
3. Tyagi S. and Kramer F. R. Molecular beacons: Probes that fluoresce upon hybridization. *Nat. Biotechnol.* 1996; **14:** 303-8.
4. Tani H., Kanagawa K., Kurata S., et al. Quantitative method for specific nucleic acid sequences using competitive polymerase chain reaction with an alternately binding probe. *Anal. Chem.* 2007; **79:** 974-9.
5. Vogelstein B. and Kinzler K. W. Digital PCR. *Proc. Natl. Acad. Sci. U.S.A.* 1999; **96:** 9236-42.
6. Pohl G. and Shie Ie M. Principle and applications of digital PCR. *Expert Rev. Mol. Diagn.* 2004; **4:** 41-7.
7. Ohler V. G., Qin J., Ramakrishnan R., et al. Absolute quantitative detection of ABL tyrosine kinase domain point mutation in chronic myeloid leukemia using a novel nanofluidic platform and mutation-specific PCR. *Leukemia* 2009; **23:** 396-9.
8. Dennis Lo Y. M., Lun F. M. F., Allen Chan K. C., et al. Digital PCR for the molecular detection of fetal chromosomal aneuploidy. *Proc. Natl. Acad. Sci. U.S.A.* 2007; **104:** 13116-21.
9. White R. A. III, Blainey P. C., Fan H. C., and Quake S. R. Digital PCR provides sensitive and absolute calibration for high throughput sequencing. *BMC Genomics* 2009; **10:** 116-27.
10. Zang Y., Novak R., Shuga J., Smith M. T., and Mathies R. A. High-performance

single cell genetic analysis using microfluidic emulsion generator arrays. *Anal. Chem.* 2010; **82:** 3183-90.

11. Sandberg S. O., Witter C. T., Gao C., and Gale B. K. Spinning disk platform for microfluidic digital polymerase chain reaction. *Anal. Chem.* 2010; **82:** 1546-50.

Chapter 5

General conclusions and perspectives

Chapter 5

General conclusions and Perspectives

5

5.1. General conclusions

Genetic markers are widely employed as diagnostics and prognostics. Novel genetic markers are now being identified by use of the exhaustive genome analysis methods such as DNA/RNA microarray and pyrosequencing. For the next stage, exploring the role of these newly found genetic markers would be progressed. Hence, the methods for detection and/or quantification of identified genetic markers are highly needed.

In this study, I aimed to develop analytical methods, which are able to cover the two types of the genetic markers. The one of the genetic marker is a type in which the mRNA is overexpressed in the particular patients. I focused on the WT1 mRNA such genetic marker. The mRNA is overexpressed in the patients with various types of leukemias but has no mutations. The expression level of the mRNA links to the conditions of the leukemia progression; therefore, the mRNA is particularly focused on the MRD monitoring of leukemia, especially in the acute type leukemias. That is because there are no highly specific genetic markers in acute type leukemias. The other has mutations and the transcripts of them trigger the diseases. I focused on JAK2V617F such genetic marker. JAK2V617F is a JAK2 gene with a point mutation in exon 14 and is a remarkable genetic marker of MPN.

In chapter 2, I described the development of two methods for the quantification of WT1 mRNA, which is the one of the remarkable genetic markers for acute leukemia. The one is real-time turbidimetry RT-LAMP that allows WT1 mRNA quantification with high specificity, simplicity, and rapidity under 62ºC within 30 min. The standard curve of the real-time turbidimetry RT-LAMP was expressed as a linear relationship between the log copy numbers of WT1 mRNA ranging from 6.8 × 10 to 6.8 × 10^9 copies and the threshold time with a correlation coefficient of $R^2 > 0.994$. The measured values obtained by real-time turbidimetry RT-LAMP strongly correlated with those obtained by real-time RT-PCR. The other is ABC RT-PCR that enables us to quantify target of the interest despite the existence of the PCR amplification inhibitors. The standard curve of the ABC RT-PCR was expressed as a sigmoid curve between the initial quantity of WT1 mRNA ranging from 10 to 10^5 copies and the relative fluorescence intensity with a correlation coefficient of $R^2 > 0.997$. The WT1 expression levels of two patients with acute leukemia correlated with the clinical events. To summarize, the pan-leukemia marker WT1 mRNA can be quantified using two novel developed methods. The RT-LAMP can be performed specifically, rapidly, and simply. Moreover, the quantitative range of RT-LAMP was found to be the same as that of real-time RT-PCR. The ABC RT-PCR has a potential to monitor the MRD of the acute leukemia. Several methods for the MRD monitoring such as the methods developed in this study would be contribute to widening the selection of the method on demand.

In chapter 3, I described the development of the simple, cost-effective, and accurate JAK2 allele burden quantification method using ABC-PCR with a slightly modification to the analytical equation. It is currently prerequisite now to quantify target JAK2 allele burden of the myeloproliferative neoplasms (MPN) patients. The standard curve by the

ABC-PCR was expressed as a linear relationship between the JAK2 allele burden ranging from 1 to 99% and the relative fluorescence intensity with a correlation coefficient of $R^2 > 0.996$. The quantification of the samples with given JAK2 allele burdens revealed that the ABC-PCR had low assay-to-assay variation at JAK2 allele burden ≥5% and that the ABC-PCR was more accurate than the TaqMan AS-qPCR ranging 10%–100% of JAK2 allele burden. The ABC-PCR can be performed to quantify target JAK2 allele burden in a single reaction by use of a conventional thermal cycler and a simple fluorometer; therefore, the throughput of the ABC-PCR is approximately twice as large and the running cost of the ABC-PCR is reduced to the half compared with TaqMan AS-qPCR. The measured JAK2 allele burdens of the MPN patients indicated approximately same values between the ABC-PCR and the TaqMan AS-qPCR. These results strongly suggest that the ABC-PCR assay would be a powerful tool for quantifying the target JAK2 allele burden.

In chapter 4, I described the construction of the standard samples for quantifying the JAK2 allele burden using digital PCR, Agilent 2100 Bioanalyzer, and NanoDrop 2000 spectrophotometer, and then the certainty of the standard was validated. The PCR products derived from UT-7 and HEL cell lines were used to construct the standard samples. The copy numbers of each PCR product were determined as different amounts between the three methods. The PCR products were mixed in different proportions, JAK2 allele burdens 1–99%, of which concentrations were 10^5 copies/μl. The standard samples were prepared based on the copy number derived from the three samples. The standard curves by the ABC-PCR obtained from the three standard series were fitted to the similar linearity. Simulating the experimental data, the maximum variation of the standard was approximately 3% at the JAK2 allele burden around 50% and the variation

was quite small (1% at most) at the high or low JAK2 allele burdens. The trend by the simulation was good agreement with the result obtained from the experiment. It is strongly suggested that the standard samples for the quantification of the nucleic acids should be checked carefully by use of plural methods. The trend will be the global standard because the validation methodology for the standard samples is not establied in the field of life science so far.

5.2. Perspectives

Candidate genetic markers will be found thick and fast in the near future. The methodology and the knowledge described in the study can be applied to almost all of the quantification of those genetic markers. Furthermore, the methods can be performed simply, accurately, and rapidly compared with the conventional nucleic acids quantification methods. Therefore, these methods will be widely employed not only in the scientific field but also in the clinical field.

In this study, I have developed the methodologies for two types of the genetic marker and have proposed how to construct the standard samples for the methods. The targeted genetic markers are the type of aberrant expression and of point mutation. However, candidate genetic markers other than these two types such as JAK2 exon 12, LNK mutations, and TET2 mutations, were identified recently. For example, JAK2 exon 12 mutational variations include the deletion and duplication of the genes in the particular regions. The variation is also thought to contribute to the development of the MPN for the same mechanism as JAK2V617F; however, the reason why these variations exist or the clinical difference between JAK2V617F and JAK2 exon 12 is unclear.

Therefore, an innovative method is desired, by which can be identified/quantified these candidates. The massively parallel genome sequencing technologies such as 454 sequencing, Solexa, and SOLiD™ system, will enable us to both identify the genomic variation and quantify the amount of such genes in the individual patient. However, these technologies require the DNA/cDNA library of which amount is rigidly identified. At this point, the plural methods for evaluating the quality of the obtained samples will be essential. Digital PCR would be the powerful tools for the purpose. On the other hand, novel methodologies for the gene specific techniques are still developed for the genetic markers that include the mutational variation. Zhang W. et al. reported the challenging trial at the 52nd American Society of Hematology (ASH) annual meeting. They have developed the combined use of the PCR fragment analysis and AS-PCR, and achieved a robust and sensitive detection of JAK2 exon 12 mutations. In the future, the next generation sequencing and the conventional gene specific quantification methods will be principal pillars for the genetic markers. Of course, the standardization of these identification/quantification methods will also be a global standard on the life science field. The procedure, the knowledge, and the proposal described in the study will contribute to the stream (Figure 5.1).

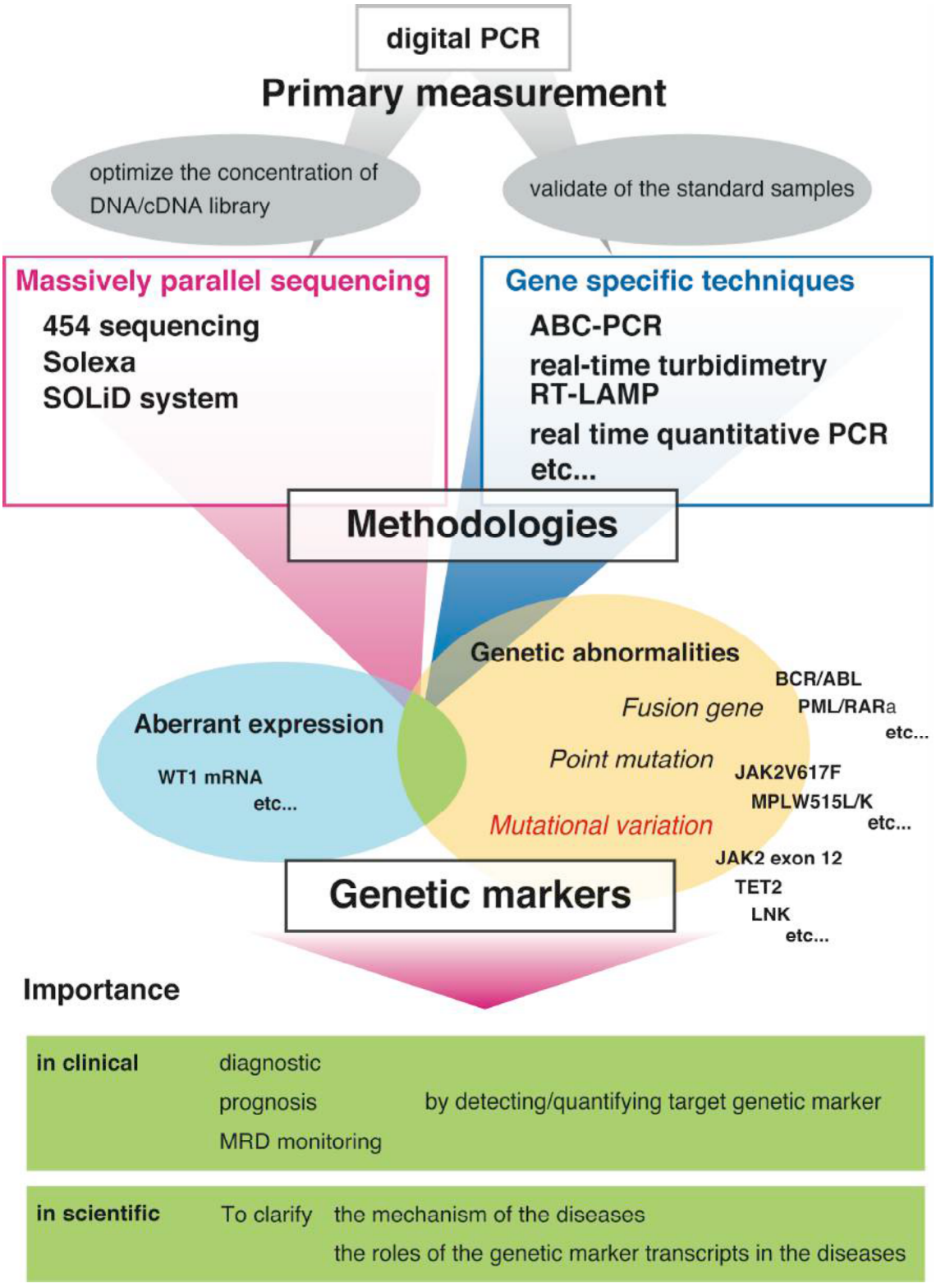

Figure 5.1. Perspective of the study

Acknowledgements

Acknowledgements

I would like to express my profound respect and gratitude to Prof. Satoshi Tsuneda (Waseda University) as my supervisor. I greatly appreciate his continuous support, timely advice, and sincere encouragement.

I would like to express my gratitude to Prof. Yasuo Ikeda (Waseda University), Prof. Takashi Kato (Waseda University), and Prof. Norio Komatsu (Juntendo University School of Medicine).

I would like to express my heartfelt gratitude to Dr. Naohiro Noda (National Institute of Advanced Industrial Science and Technology (AIST)) for giving me a chance to study in AIST in Tsukuba and helpful advice and encouragement throughout the study.

I would like to express my gratitude to Dr. Kazunori Nakamura (AIST and J-Bio 21 Corp.), Dr. Yuji Sekiguchi (AIST), and Prof. Keita Kirito (University of Yamanashi) for constructive and useful comments.

I am thankful to Dr. Shinya Kurata (J-Bio 21 Corp.), Mr. Hidekazu Sogo (J-Bio 21 Corp.) for constructive comments and warm encouragement.

I am very grateful to all the members in the Bio-measurement Research Group and Microbial and Genetic Resources Research Group in AIST, particularly Ms. Chiiko Sakai, Ms. Sachiko Imai and Ms. Yukiko Narihiro for secretarial contribution, and Ms. Akiko Ohashi and Ms. Satowa Yoshi-ike for experimental supports.

I appreciate to Ms. Mariko Ozawa, Ms. Hidemi Yamazoe, Ms. Mirai Iwaya (Department of Hematology/Oncology, University of Yamanashi), Ms. Kyoko Kubo (Department of Hematology, Juntendo University School of Medicine) and Dr. Aya H. Koda (the former Assistant Professor in Juntendo University School of Medicine) for their technical assistance.

I am very grateful to all the colleagues in AIST, particularly Dr. Ryo Miyata, Dr. Hidenori Tani, Dr. Ken Adachi, Mr. Hitoaki Tabo, Ms. InWoo Bae, Mr. Tatsuya Teramura, Ms. Nao Morita, Mr. Masahiro Yamaguchi, Ms. Yuka N. Kato, Mr. Osamu Fujita, Mr. Yasuyoshi Matsuda, Mr. Atsushi Furuta, and Ms. Mayu Toyonaga.

I thank to all the members of Tsuneda Laboratory, particularly Ms. Hiroko Takeno, Ms. Akiko Sano, Dr. Yuki Kagawa, Dr. Yoshiteru Aoi, Dr. Tatsuhiko Hoshino, Dr. Sachiko Yoshie, Dr. Akihiko Terada, Dr. Takashi Kondo, Dr. Naohiro Kishida, Dr. Toshifumi Osaka, Dr. Takeshi Terahara, Dr. Kazuhiro Furukawa, Dr. Shinya Matsumoto, Dr. Yasuhiro Date, Ms. Haruko Obokata, and Mr. Hirotsugu Fujitani.

Finally, I would like to express my profound gratitude to my family. I would not be able to complete this thesis without their helps and encouragements.

February 2011

Soji Morishita

Appendices

博士論文概要

バイオマーカーは，生体の特定の疾病の存在や状態の指標となる物質を指し，核酸，ペプチド，タンパク質，脂質代謝物等，対象は多岐にわたる。なかでも核酸由来バイオマーカー（遺伝子マーカー）は遺伝子定量手法の発展・普及により比較的簡便に検出あるいは定量できるため，病態の診断，治療の予後予測，病態のモニタリングに利用されるなど，臨床の現場へ着実に応用されつつある。このような試みは，がん分野において積極的に行われているが，特に血液疾患における進歩はめざましく，他のがん分野を常に牽引してきた。例えば，慢性骨髄性白血病（chronic myeloid leukemia：CML）患者の 90%以上に，CML の遺伝子マーカーである BCR/ABL キメラ遺伝子が存在することが知られている。BCR/ABL キメラ遺伝子は CML 診断の極めて有効な指標であるばかりか，BCR/ABL キメラ遺伝子の ABL キナーゼドメインにおける点突然変異の有無や種類が薬剤選択の指標となるため，治療の予後予測が立てやすい。さらには，BCR/ABL キメラ遺伝子量を定量することで，治療の経過を容易にモニタリングできる。

これまで述べてきたように，遺伝子マーカーは病態の診断・判定の指標としての利用に留まらず，治療の予後予測，病態のモニタリングなどにも利用されており，今後，新たな遺伝子マーカーの探索・同定，および同定された遺伝子マーカーの検出・定量技術は重要な位置を占めると考えられる。事実，近年，網羅的な遺伝子解析，ゲノム解析を可能とする様々な手法が確立され，それらを用いた解析により，新たな遺伝子マーカーが次々と発見・報告されている。それに伴い，病態診断の拠り所として，また，治療の予後予測や病態モニタリングの手段として，遺伝子マーカーの定量の必要性が高まっている。そこで，本研究では造血器腫瘍関連，特に白血病と骨髄増殖性腫瘍の遺伝子マーカーを定量するための新規な遺伝子定量技術の確立を目的とした。

本論文は 5 章から構成されている。以下に各章の概要について述べる。

第 1 章では，造血器腫瘍の遺伝子マーカーと，その検出・定量技術に関する既往の知見および問題点を，最近の研究動向を踏まえつつ概説し，本研究の研究背景をまとめるとともに，本研究の意義および目的を明らかにした。

第 2 章では，白血病（特に急性白血病）の汎用遺伝子マーカーとして臨床検査へ実用化された Wilms Tumor 1 mRNA（WT1 mRNA）の発現量を，既存手法と比較し，より迅速，簡便に定量するための新たな定量系を確立した。まず，reverse transcription loop-mediated isothermal amplification（RT-LAMP）法を用い，WT1 mRNA の迅速・簡便な定量系を構築した。RT-LAMP 法は reverse transcription polymerase chain reaction（RT-PCR）法のように温度変化を必要とせず，等温条件下で対象遺伝子を増幅可能な新規遺伝子増幅手法である。また，RT-PCR 法では RNA の逆転写反応とその後の増幅反応を別々に実施する必要があるのに対し，RT-LAMP 法は等温反応であるため，逆転写反応と増幅反応が同時に起こり，比

較的短時間で反応が終了するという利点を有する。さらに，遺伝子増幅反応の副産物であるピロリン酸マグネシウムの生成量を濁度としてリアルタイムに測定することで,対象の遺伝子量を定量することも可能である。このような利点により，RT-LAMP 法を WT1 mRNA 定量へ応用できれば，迅速・簡便な白血病の病態モニタリングが可能になると期待される。WT1 mRNA を特異的に増幅させるような短鎖 DNA オリゴ（プライマー）のセットを設計し，それらを用いて RT-LAMP 法による WT1 mRNA の増幅を試みたところ，10 コピーの WT1 mRNA を 30 分程度で検出できた。さらに，HeLa 株抽出 RNA に WT1 mRNA を既知量混入させたものを測定用サンプルとして調整し，これらサンプル中の WT1 mRNA 量を RT-LAMP 法およびリアルタイム RT-PCR 法でそれぞれ定量した。その結果，両手法とも真値に近い値を示すことが明らかとなった。これらの結果により，RT-LAMP 法はリアルタイム RT-PCR 法と同等の定量精度を持ちながらもより迅速・簡便に白血病の病態をモニタリングできる手法であることが示唆された。つづいて，より正確な病態モニタリング実現のため，遺伝子の増幅阻害物質混入下でも正確な遺伝子定量が可能な手法である Alternately Binding probe Competitive（ABC）法を RT-PCR 法と組み合わせ（ABC RT-PCR 法），WT1 mRNA の簡便・正確な定量手法の確立を試みた。ABC RT-PCR 法では，対象となる遺伝子と等しい増幅効率で競合的に増幅される内部標準遺伝子を既知量，反応系に添加し，反応を行う。反応系にはグアニン塩基との電子移動により蛍光強度が著しく消光する性質を持った蛍光色素がラベルされたプローブが添加されており，増幅反応後の蛍光強度が対象遺伝子と内部標準遺伝子の割合を反映するため，対象遺伝子量を算出できる。本手法最大の特長は内部標準法であるために遺伝子の増幅阻害物質の影響を数学的に打ち消すことのできる点であり，既存手法と比較して，より正確な定量が可能となる。急性白血病患者２名より経時的に採取した骨髄サンプルよりトータル RNA を抽出し，これらのサンプル中の WT1 mRNA 発現量を ABC RT-PCR 法にて定量したところ，各々の患者の病態に従って WT1 mRNA 発現量が増減する様子が確認され，ABC RT-PCR 法により白血病の病態モニタリングが可能であることが示唆された。

第３章では，骨髄増殖性腫瘍（myeloproliferative neoplasm : MPN）において 2005 年に報告された遺伝子マーカーである Janus Kinase 2（JAK2）遺伝子の点突然変異（JAK2V617F）のアレルバーデン（(変異 JAK2 遺伝子量／JAK2 全遺伝子量）×100%）について，簡便・低コスト・正確な定量手法の構築を行った。第２章にて触れた ABC 法を PCR 法と組み合わせ（ABC-PCR 法），JAK2 アレルバーデン定量へ応用することにより，既存の手法と比較して，より簡便に低コストで，かつ，正確に対象の JAK2 アレルバーデンを定量することが可能である。ABC-PCR 法では，増幅反応後の蛍光値が対象のアレルバーデンに依って変化するため，PCR 法により対象の DNA を増幅し，その後に蛍光強度を測定するのみで対象の JAK2 アレルバーデンを定量することが可能である。また，スループットが既存手法であるリアルタイムアリル特異的 PCR（リアルタイム Allele Specific PCR : リアルタイム AS-PCR）法の約２倍であるため，ランニングコストをおよそ半分に抑え

ることができる。ABC-PCR 法の定量精度確認のため，UT-7 株（JAK2 野生型株）抽出 DNA と HEL 株（JAK2 変異型株）抽出 DNA を任意のアレルバーデンとなるように混合し，模擬定量サンプルを調整した。これらの JAK2 アレルバーデンを ABC-PCR 法とリアルタイム AS-PCR で定量し，その値を真値と比較した。その結果，ABC-PCR 法はアレルバーデン≥10%の範囲においてリアルタイム AS-PCR よりも真値をよく反映した値を示し，リアルタイム AS-PCR はある程度の真値からのずれを許容すればアレルバーデン下限値 1%まで定量可能であるという結果を得た。これにより，ABC-PCR 法は定量下限においては既存手法に劣るが，アレルバーデン≥10%の範囲では，既存手法よりも正確に対象のアレルバーデンを定量可能であることが示唆された。最後に，MPN 患者と健常者より採取した血液サンプルより DNA を抽出し，それらのサンプル中の JAK2 アレルバーデンを ABC 法，リアルタイム AS-PCR 法でそれぞれ定量し，その値を比較した。その結果，アレルバーデン下限値 10%までにおいて両者の定量結果には相関性があった。これにより，ABC-PCR 法は既存手法と比較し，アレルバーデン≥10%の範囲では，簡便・低コスト・正確に対象の JAK2 アレルバーデンを定量できる手法であることが示された。

第 4 章では，第 3 章にて確立した ABC-PCR 法による JAK2 アレルバーデン定量のための標準サンプルの作製・評価手法を提案した。近年，標準曲線を用いた相対的な定量（相対定量）ではなく，直接的な定量（絶対定量）によって対象の遺伝子数を測定する新たな手法（デジタル PCR 法）が確立された。本手法により，対象の遺伝子数やアレルバーデンを直接定量することが可能であるが，ランニングコストの高さとスループット性の低さから，定量系としての実用化は難しい。そこで，デジタル PCR 法をアレルバーデンの値を保証された標準サンプル作製のために運用することを考えた。これによって，コストを最小限に抑えつつ，定量の正確性を担保できると期待される。まず，AS-PCR を基盤としてデジタル PCR 法により JAK2 アレルバーデンを定量できるような反応条件を検討した。つづいて，これを用いて野生型 JAK2 遺伝子量と変異型 JAK2 遺伝子量をデジタル PCR 法で定量し，その定量値をもとに ABC-PCR のための標準サンプルを作製した。最後に，作製した標準サンプルを用いて ABC-PCR 法を実施し，アレルバーデンの真値を忠実に反映した定量結果を得られることを確認した。

第 5 章では本論文を総括した。

以上，本論文では造血器腫瘍，特に急性白血病と骨髄増殖性腫瘍の遺伝子マーカーを簡便・低コスト・正確に検出・定量できる手法の確立を行った。本成果は今後さらに発見がなされてゆくものと予想される種々の遺伝子マーカーの検出・定量へも応用可能であり，臨床検査医学の分野に大きく寄与できるものと期待される。

研究業績

【論文】

(1) （報文）Hidenori Tani, Ryo Miyata, Kouhei Ichikawa, Soji Morishita, Shinya Kurata, Kazunori Nakamura, Satoshi Tsuneda, Yuji Sekiguchi, and Naohiro Noda, Universal quenching probe system: flexible, specific, and cost-effective real-time PCR method, *Analytical Chemistry* 2009; **81:** 5678-5685.

(2) （報文）Soji Morishita, Hidenori Tani, Shinya Kurata, Kazunori Nakamura, Yuji Sekiguchi, Satoshi Tsuneda, and Naohiro Noda, Real-time reverse transcription loop-mediated isothermal amplification for rapid and simple quantification of WT1 mRNA, *Clinical Biochemistry* 2009; **42**: 515-520.

【講演（国際会議）】

(1) Soji Morishita, Naohiro Noda, Yuji Sekiguchi, Aya H. Koda, Yuriko Yahata, Keita Kirito, Satoshi Tsuneda, and Norio Komatsu, Alternately Binding Quenching Probe Competitive PCR: Simple, Sensitive, and Cost-Effective JAK2 Allele Burden Quantification Method, The 52nd ASH annual meeting, Orlando, FL, USA, December 2010.

【講演（国内）】

(1) 森下 総司, 谷 英典, 蔵田 信也, 中村 和憲, 常田 聡, 関口 勇地, 野田 尚宏,
RT-LAMP 法を用いた白血病マーカーWT1 mRNA の迅速・簡便定量技術の開発, 化学工学会第 74 年会, 横浜, 2009 年 3 月

(2) 森下 総司, 谷 英典, 蔵田 信也, 中村 和憲, 常田 聡, 関口 勇地, 野田 尚宏,
Reverse transcription loop-mediated isothermal amplification (RT-LAMP)法を用いた白血病マーカーWT1 mRNA の迅速・簡便定量技術の開発, 第 60 回生物工学会大会, 仙台, 2008 年 8 月

(3) 森下 総司, 谷 英典, 寺村 達也, 足立 賢, 常田 聡, 蔵田 信也, 中村 和憲, 金川 貴博, 関口 勇地, 野田 尚宏, 新規遺伝子定量手法 ABC-LAMP 法の開発, 化学工学会関東・東北・北海道合同支部大会, 東京, 2007 年 11 月

【その他】

(1) （特許）野田 尚宏，関口 勇地，森下 総司，常田 聡，小松 則夫，蓮沼 彩，桐戸 敬太，JAK2遺伝子の変異解析方法，特願2010-174571

(2) （新聞掲載）白血病，30分で症状把握，日経産業新聞，2008年8月

(3) （受賞）平成 19 年度化学工学会学生賞，2007 年 11 月

謝辞

本研究ならびに本論文の作成は，早稲田大学先進理工学研究科生命医科学専攻常田研究室にて行われました。本研究を進めるにあたり，お世話になった方々にこの場を借りて感謝の意を表します。

本研究を進めるにあたり，終始あたたかくご指導くださいました常田聡教授に心から深く感謝いたします。

本研究をまとめるにあたり，早稲田大学理工学術院　池田康夫教授，同大学教育・総合科学学術院　加藤尚志教授，順天堂大学医学部血液内科　小松則夫教授には副査の立場から貴重なご教示とご助言をいただきました。厚く御礼申し上げます。

産業技術総合研究所バイオメディカル研究部門バイオメジャー研究グループ研究員の野田尚宏博士には，実質的な研究の進め方から日々の研究活動に至るまで，常に貴重なご指導をいただき，親身になって研究生活を支えていただきました。謹んで感謝申し上げます。

産業技術総合研究所バイオメディカル研究部門研究顧問の中村和憲博士，同研究部門バイオメジャー研究グループリーダーの関口勇地博士，山梨大学医学部血液・腫瘍内科の桐戸敬太教授には，研究に対するフィロソフィーから論文の作成に至るまで，大変貴重なご指導をいただきました。心より感謝申し上げます。

産業技術総合研究所秘書の酒井ちい子さん，今井左知子さん，成廣由紀子さん，同研究所技術補助員の大橋明子さん，吉池里和さん，内藤（旧姓加藤）有香さんを初めとするバイオメディカル研究部門バイオメジャー研究グループ，生物プロセス研究部門生物資源情報基盤研究グループの皆様には，日々の研究の遂行にあたり，多大なご協力と激励をいただきました。

山梨大学医学部血液・腫瘍内科秘書の小澤満里子さん，技術補助員の山添秀美さん，岩谷未来さんをはじめとする同大学血液・腫瘍内科医局員の皆様，順天堂大学医学部血液内科秘書の久保恭子さん，元・同大学医学部特任助教の蓮沼（旧姓甲田）彩博士を初めとする順天堂大学医学部血液内科医局員の皆様には，慣れない環境での研究生活を支えていただきました。

産業技術総合研究所にて研究生活を共にした，常田研究室の谷英典博士（現・東京大学アイソトープ総合センター研究開発部秋光研究室博士研究員），足立賢博士（現・古河電工），寺村達也氏，森田奈央さん，山口正裕氏，藤田統氏，松田泰嘉氏，古田篤史氏，DNA チップ研究所の宮田亮博士，長岡技術科学大学大学院工学研究科環境システム専攻の豊永真由さんには，公私ともに多大なるご助力と励ましをいただきました。

常田研究室秘書の武野弘子さん，佐野晶子さん，加川友己博士，青井議輝博士，星野辰彦博士，吉江幸子博士，寺田明彦博士，近藤貴志博士，岸田直裕博士，大坂利文博士，寺原猛博士，古川和寛博士，松本慎也博士，小保方晴子氏をはじめとする常田研究室の皆様には，日々の研究の遂行にあたり，あたたかい励ましや，大変有意義な意見をいただきました。

こうした皆様をはじめとする，様々な方々の協力によって本研究を無事成就することができました。改めて心から厚く感謝申し上げます。

最後に，常に私の行動を温かく見守り，惜しみなく援助してくださった家族に心から厚く御礼申し上げます。

2011 年 2 月

森下　総司